

1 *We would like to acknowledge the time and effort that Editor Dr. Helen McGregor, 2k Special*
2 *Issue Data Review Team, and the two anonymous reviewers have put into assessing the*
3 *previous version of the manuscript. We have provided the responses to each of the editors'*
4 *and reviewers' comments below. These are shown in blue italics. At the end of this document,*
5 *we also provide a version of the manuscript where all changes are marked in yellow.*

6 *We look forward to hearing from you in due time regarding our resubmission and to respond*
7 *to any further questions and comments you may have.*

8 *On behalf of the authors,*

9 *Kristina Seftigen*

10 -----
11 **Dr Helen McGregor**

12 Regarding your request for clarification on the referee #1 comment:

13 "Sec./Fig. S1: I'm a bit lost here. How can the annual mean be overestimated if all monthly
14 means are underestimated?" All that is required is to clarify that the data in Fig. S1b are from
15 southern Scandinavia (not stated in the caption or text as far as I can tell).

16 *Response: done*

17
18 In addition, in response to Referee #2's point 1., I encourage you to consider adding to the
19 methods the more specific context you provide in your response (text could be inserted
20 around the callout for Figure S3). Although the use of TRW to moisture balance is discussed
21 in general terms in the introduction the additional text in the methods will assist readers to
22 recognise the importance of the data presented in Figures S3 and S6.

23 *Response: thank you for this suggestion. The text is now added (lines 122-137).*

24
25 **Referee #1**

26 In general I find some formulations too strong and not fully supported by the presented
27 analysis. This is in particular the case for formulations of over/underestimation and biases in
28 the model output in comparison to the SPEI reconstruction. When comparing two non-perfect
29 representations of a variable these terms are in my view only justified if one also includes
30 observational data or if there is compelling evidence that one of the two is a better
31 representation of physical reality. At most parts of the manuscript suggests that the proxy
32 reconstruction is an accurate representation and the discrepancy is mainly due to an inability
33 of the GCMs to reproduce these features. A better way would be, to just state a difference in
34 variability, possibly followed by an assessment of both representations. The authors state in
35 lines 561-562, that it is not possible to attribute the disagreements between the reconstruction
36 and the models to one side. This is in disagreement with the rest of the paper, which blames
37 the models. A reasonable formulation is found in lines 544-547 and I would have liked to see
38 similar remarks earlier in the text.

39
40 This can probably be easily resolved by reformulating certain statements. In the current form,
41 I found it widely irritating while reading. Some examples of statements which I find too
42 strong (there might be others) are:

43
44 - l. 19-20, l. 315-318, l. 460-465 and l. 532-533: I would like to see a critical assessment of
45 the variability of the SPEI reconstruction and a deeper comparison to the expected time-scale
46 depended variability, also from observational data. Just comparing the model output to the

47 reconstruction is in my view not enough to conclude a bias on the model-side.

48

49 - l. 22-23, l. 520-522: The formulation implies, that a positive correlation on multidecadal
50 scales is also found from observational evidence. This is not provided in the manuscript, but
51 is crucial to determine if the mismatch between proxies and models is mainly due to GCMs
52 deficiencies. Thus, much of the paragraph l. 518-526 is formulated with a bias towards a
53 correct representation in the proxy reconstruction. The fact, that the multi-decadal variability
54 is much stronger in the reconstructions can have many reasons (some of which are also
55 discussed in the manuscript), but to claim a bias in the models from this fact alone is a bit
56 strong.

57

58 *Response: we agree with the reviewer that some of the statements are perhaps formulated too*
59 *strong. Following the reviewer suggestions we have now reformulated some of the text.*
60 *Rather than attributing the mismatch to either of the datasets, sect. 3 and 5 are now more*
61 *focused on describing the inconsistencies in the model and proxy records. Possible causes of*
62 *the disagreement are briefly discussed in the final sect. 'summary and discussions'. The*
63 *abstract has been rephrased accordingly.*

64

65 - l. 215-216: It is not immediately clear, which period is the validation and which is the
66 calibration period.

67

68 *Response: We have used a split period calibration/validation procedure, which means that*
69 *both the early (1901-1948) and the late (1949-1995) periods have been used for calibration*
70 *and validation. A more detailed description of the calibration/validation scheme (l.198-202)*
71 *is now provided.*

72

73 - Fig 3: It would be nice to include (at least for the high-frequency part) observations into this
74 plot, to be able to judge both the proxy and the model performance. In Fig. 3 (d), adding the
75 markers to the legend would make it more intuitive to read, especially for monochromatic
76 prints.

77

78 *Response: Thank you for the suggestion. We have now provided observational data in the*
79 *comparison. Also, the legend in fig. 3d is changed as suggested.*

80

81 - Fig 4.: I found it a bit confusing that the order of the columns does not correspond to the
82 order in which the variables are discussed in the text. I would recommend adjusting the order
83 accordingly.

84

85 *Response: Order revised*

86

87 - Repeatedly the formulations seem to imply that hydroclimate and temperature/ precipitation
88 are independent variables which one can "contrast" or "compared" (e.g. l. 227). While the
89 first is rather a combination of the two and thus one is not comparing them, but rather
90 investigating, which factor is more dominating.

91

92 *Response: Agreed, the text is now revised.*

93

94 - As a reader who is not familiar with SPEI it is hard to follow what this variable does and
95 what it's dependencies are. I would have liked to see the formula that is used in this study,
96 possibly in the Supplementary Material.

97
98
99
100
101
102
103
104
105
106
107
108
109
110
111
112
113
114
115
116
117
118
119
120
121
122
123
124
125
126
127
128
129
130
131
132
133
134
135
136
137
138
139
140
141
142
143
144
145
146

Response: Thank you for this suggestion. A more detailed description of the SPEI computation, as well as some technical notes on the use of the SPEI R package, are now provided in the supplementary materials.

- l. 235-236: While the two time series are coming from different data sets they might still share common signals and might not be totally independent. Given the rather low r^2 of 0.2, one could also argue that the low-frequency variability of the SPEI index, which is a combination of precipitation and temperature, is simply dominated by the temperature component, which would lead to similar multi-decadal variability with ScandT14.

Response: We thank the reviewer for his/her comment. We however argue that one would expect the two reconstructions ScandH17 and ScandT14 to be anti-correlated in the decadal/lower frequencies (warm decades -> dry decades), would the low-frequency portion of the reconstructed SPEI series be dominated by a temperature component. Interestingly, this is not the case. We have showed in the manuscript that a precipitation signal dominates the high-frequency portion of the TRW variability. Theoretically one would therefore expect the decadal variability to also be driven by changes in rainfall rather than temperature. However, we cannot rule out that there might be a frequency dependent sensitivity of the proxy data to climate and that the influence of temperature could increase towards lower frequencies of the spectra. We have now discussed this issue in lines 581-584.

- l. 309/310: A reference to the Supplementary Material Sec. S1 could strengthen this claim, even though it only applies to the inter-annual time scale.

Response: done.

- Sec. 4: I found the title misleading, as the only external forcing discussed is volcanic eruptions, while other forcings like solar variability are not mentioned. Please revise the title.

Reply: the header is now revised to 'The role of volcanic forcing'

- l. 432 ff: I found this paragraph a bit confusing. While it begins with comparison of temperature and precipitation the results are about temperature and SPEI. As SPEI is a mixed variable, which also includes temperature, it is not clear, how one can draw a connection to a T-precip relationship. In general, it seems like SPEI and precipitation are used interchangeable here, which they are not.

Response: The SPEI and precipitation have here been used interchangeable because there is presently no high-resolution, fully independent proxy reconstruction of rainfall available for the region. Also, we show that the SPEI variability is dominated by a precipitation signal in the region (Fig. S5). However, we agree that some of the readership might find this section a bit confusing. We have therefore revised the text (l.444-467), to be more focused on the role of temperature in regional hydroclimate. We have also added two new plots to the supplementary materials (Fig. S9), that are more closely exploring the association between simulated SPEI, temperatures and rainfall across different frequency bands.

- l. 448 ff: Can you quantify the relationship between ScandH17 and ScandT14? While the multi-decadal co-variability is clearly visible by eye this is not the case for the interannual values. In both cases it would be nice to have quantified values (including significance).

Reply: done (l.453 and l.458).

147
148 - Sec./Fig. S1: I'm a bit lost here. How can the annual mean be overestimated if all monthly
149 means are underestimated?

150 *Reply: We are not sure that we understand the referees' comment. Fig S1b is based on model*
151 *data from southern Scandinavia, where many of the models underestimate the annual rainfall*
152 *(blue areas in fig. S1a).*

153

154 Technical Corrections

155 - 387 [. . .] superior [to] TRW [. . .]

156 *Reply: corrected*

157 **Referee #2**

158 1. The growth of tree-ring width (TRW) may be limited by the shortage of water. However,
159 does the TRW positively and linearly depend on soil moisture/ precipitation? Can TRW
160 proxies reflect floods/extreme wetness, especially when the study region is not arid?

161 *Response: We thank the reviewer for taking time to review our manuscript and providing us*
162 *with a number of valuable and insightful comments and suggestions. We understand that the*
163 *use of TRW data from moist and cool Scandinavia in moisture/rainfall reconstructions might*
164 *appear controversial to some readers. After all, the developments of moisture sensitive TRW*
165 *data have traditionally been restricted to lower latitude arid and semi-arid regions, with only*
166 *a few exceptions for the northern European sector. Yet, we argue that moisture stressed trees*
167 *do grow in these high-latitude environments and tree-ring chronologies with moisture*
168 *sensitivity can be developed, at least if species and sites are carefully selected, which has also*
169 *been proven by a number of recent studies (Helama & Lindholm, 2003; Wilson et al., 2012;*
170 *Cook et al., 2015 etc.). In our study, we have almost exclusively used TRW data from sites*
171 *with shallow and well-drained soils - that is, sites where the growth of vegetation is clearly*
172 *affected by the amount of available moisture. We have therefore been able to build*
173 *chronologies that are positively and more strongly correlated with moisture availability than*
174 *with temperature variability, which is demonstrated in figs S3 and S6 in the supplementary*
175 *materials.*

176

177 2. I see you have another field hydrological reconstruction over Fennoscandia based on much
178 more proxy records. Have you compared this reconstruction with that one over Scandinavia?
179 Is there any difference for the northern part?

180 *Response: yes, in Seftigen et al. (2014) we have used a denser tree-ring network to provide a*
181 *field reconstruction over much of Fennoscandia. In that study the tree-ring data from the*
182 *northernmost parts of Fennoscandia were mostly negatively correlated with available*
183 *moisture and therefore we used it indirectly to reconstruct soil moisture availability, by*
184 *considering the importance of surface temperature in determining the land surface heat flux,*
185 *evapotranspiration and consequently the water balance. Mixing tree-ring data with different*
186 *signals for reconstruction purposes is however not always straightforward, and as the main*
187 *aim of the current study was to provide as robust and reliable reconstruction for the region*
188 *we decided to only retain tree-ring data from moisture stressed sites, where the tree-growth is*
189 *positively related to drought. As is shown in the manuscript fig 1, these sites are mainly*
190 *located in southern Sweden. Comparing the current reconstruction with the 2014*
191 *reconstruction would yield basically the same results over southern Sweden, as the two*
192 *reconstructions share more or less the same set of predictors in this region. The only*
193 *difference would be that the current reconstruction contains more low-frequency information*
194 *than the 2014 reconstruction (see sect. 2.2 in the manuscript). We have not compared the new*

195 *reconstruction with the previous one over northern Sweden, simply because the signal of the*
196 *new reconstruction is confined to southern and central Scandinavia (see fig. 1).*

197
198 3. The comparison between the reconstruction and the simulations is interesting. However
199 some conclusions, from my point of view, are too strong. For example, “We find simulated
200 interannual components of variability to be overestimated, while the multidecadal/longer
201 timescale components generally are too weak.” I supposed the conclusion is drawn from the
202 lines from 307-322. As far as I understand, the TRWs tend to have red biased spectra, please
203 see the papers from Franke et al. (2013) and Bunde et al. (2013). So, is it possible that the
204 TRW-based reconstruction overestimated low-frequencies? If that is the case, then the
205 following conclusions are not solid. Especially, “Weak multidecadal variability in models
206 also implies that inference about future persistent droughts and pluvials based on the latest
207 generation global climate models will likely underestimate the true risk of these events.”

208 *Response: We agree that some of the statements were made a bit too strong – it is true that we*
209 *are currently unable to identify the precise origin of the mismatch. We have now revised the*
210 *manuscript to be more focused on highlighting the discrepancies in the datasets rather than*
211 *drawing any conclusion about the source for the mismatch (see response to referee #1).*

212

213 **2k Special Issue Data Review Team**

214 (1) Expand the "Data Availability" section to include a Data Citation or URLs to the primary
215 output of this study (regional SPEI nested reconstruction (ScandH17) and the 100-year
216 smooth and estimate uncertainty).

217

218 (2) Add Data Citations or URLs (in addition to publication citations) for each of the 27 tree-
219 ring chronologies used in this study to Table II (we note that Table II includes only 25 entires).
220 For those raw data not already in a persistent public repository, submit the essential metadata
221 along with the chronology itself and add the corresponding Data Citation (or URL) in Table II.
222 The archived data must contain the modified chronologies as they were re-processed and used
223 in this study (newest signal-free standardization; adjusted to reduce variance bias). The
224 ‘Updated by Seftigen et al. 2015’ revisions should be publicly archived and the ‘Seftigen et al.
225 2015’ datasets should also be archived.

226

227 (3) Add a Data Citation for the ScandT14 reconstruction (Fig 7a). If the data have not
228 previously been deposited in a public data repository, then submit the essential metadata
229 along with the time series itself and add the corresponding Data Citation and publication
230 citation to the caption for Fig 7.

231 *Response: The ScandT14 reconstructions will be made available through the NOAA*
232 *paleoclimate database, and citation will be added to the paper. Metadata, including all new*
233 *chronologies, re-processed chronologies as well as the new ScandH17 reconstruction*
234 *(smoothed and raw), will be added to supplementary materials.*

235

236 **References:**

237 Cook, E.R., Seager, R., Kushnir, Y., Briffa, K.R., Büntgen, U., Frank, D., Krusic, P.J., Tegel, W., van
238 der Schrier, G., Andreu-Hayles, L., Baillie, M., Baittinger, C., Bleicher, N., Bonde, N.,
239 Brown, D., Carrer, M., Cooper, R., Čufar, K., Dittmar, C., Esper, J., Griggs, C., Gunnarson,
240 B., Günther, B., Gutierrez, E., Haneca, K., Helama, S., Herzig, F., Heussner, K.-U., Hofmann,
241 J., Janda, P., Kontic, R., Köse, N., Kyncl, T., Levanič, T., Linderholm, H., Manning, S.,
242 Melvin, T.M., Miles, D., Neuwirth, B., Nicolussi, K., Nola, P., Panayotov, M., Popa, I., Rothe,
243 A., Seftigen, K., Seim, A., Svarva, H., Svoboda, M., Thun, T., Timonen, M., Touchan, R.,
244 Trotsiuk, V., Trouet, V., Walder, F., Ważny, T., Wilson, R. & Zang, C. (2015) Old World
245 megadroughts and pluvials during the Common Era. *Science Advances*, **1**

246 Helama, S. & Lindholm, M. (2003) Droughts and rainfall in south eastern Finland since AD 874,
247 inferred from Scots pine tree-rings. *Boreal Environment Research*, **8**, 171-183.
248 Seftigen, K., Björklund, J., Cook, E.R. & Linderholm, H.W. (2014) A tree-ring field reconstruction of
249 Fennoscandian summer hydroclimate variability for the last millennium. *Climate Dynamics*,
250 **44**, 3141-3154.
251 Wilson, R., Miles, D., Loader, N.J., Melvin, T., Cunningham, L., Cooper, R. & Briffa, K. (2012) A
252 millennial long March–July precipitation reconstruction for southern-central England. *Climate*
253 *Dynamics*,

254

255

256

257

258

259

260

261

262

263

264

265

266

267

268

269

270

271

272

273 **Hydroclimate variability in Scandinavia over the last millennium - insights from a**
274 **climate model-proxy data comparison**

275 Kristina Seftigen^{1,2,*}, Hugues Goosse², Francois Klein², Deliang Chen¹

276 ¹Regional Climate Group, Department of Earth Sciences, University of Gothenburg, Gothenburg, Sweden.

277 ²Georges Lemaître Centre for Earth and Climate Research (TECLIM), Earth and Life Institute, Université
278 catholique de Louvain (UCL), Belgium.

279 *Corresponding author:

280 E-mail address: kristina.seftigen@gvc.gu.se

281 **Abstract**

282 The integration of climate proxy information with General Circulation Model (GCM)
283 results offers considerable potential for deriving greater understanding of the mechanisms
284 underlying climate variability, as well as unique opportunities for out-of-sample evaluations
285 of model performance. In this study, we combine insights from a new tree-ring hydroclimate
286 reconstruction from Scandinavia with projections from a suite of forced transient simulations
287 of the last millennium and historical intervals from the CMIP5 and PMIP3 archives. Model
288 simulations and proxy reconstruction data are found to broadly agree on the modes of
289 atmospheric variability that produces droughts/pluvials in the region. Despite these dynamical
290 similarities, large differences between simulated and reconstructed hydroclimate time series
291 remain. We find that the GCMs simulated multidecadal/longer hydroclimate variability is
292 systematically smaller than the proxy based estimates, whereas the dominance of GCM
293 simulated high-frequency components of variability is not reflected in the proxy record.
294 Furthermore, the paleoclimate evidence indicates in-phase coherencies between regional
295 hydroclimate and temperature on decadal time-scales, i.e. sustained wet periods have often
296 been concurrent with warm periods and vice versa. The CMIP5/PMIP3 archive suggests, on
297 the other hand, out-of-phase coherencies between the two variables in the last millennium.
298 The lack of adequate understanding of mechanisms linking temperature and moisture supply
299 on longer time scales has serious implications for attribution and prediction of regional
300 hydroclimate changes. Our findings stresses the need for further paleoclimate-data model
301 intercomparison efforts to expand our understanding of the dynamics of hydroclimate
302 variability and change, to enhance our ability to evaluate climate models, and to provide a
303 more comprehensive view of future drought and pluvial risks.

304 **1. Introduction**

305 Among the current key priorities in climate research is a more comprehensive understanding
306 of changes in regional- to continental-scale hydroclimate in response to rising levels of
307 atmospheric greenhouse gases on time scales ranging from decades to centuries (Wu et al.,
308 2013; Hegerl et al., 2015). Delineating the role of internal variability and natural forcing, and
309 its contribution to the anthropogenically forced twentieth century climate (Zhang et al., 2007;
310 Sarojini et al., 2016), is immensely important for attributing past and predicting future
311 trajectories in the hydrological cycle, and for strategic approaches to adaptation and planning.
312 Sparse observational evidences limits possibilities of providing tight constraints on the long-
313 term behavior of the climate system. The longest instrumental records (~150-200 years) are
314 too short to fully sample modes of variability that are either rare or occur on multidecadal-to-
315 centennial timescales. This motivates the development of paleoclimatic proxy reconstructions,
316 which extends the observational baseline into the longer spectrum of climate variability and
317 provides a framework to consider both internal and forced climate changes.

318 Considerable advancements have recently been made in developing tree-ring
319 estimates of late Holocene hydroclimate variability across Scandinavia (Seftigen et al., 2014;
320 Cook et al., 2015). Being located in the high-latitude boreal zone, Scandinavia is well suited
321 for dendroclimatological studies and has a long tradition of climate and environmental
322 research using tree-ring data (Linderholm et al., 2010). The use of tree-ring proxy evidence to
323 study natural hydroclimate variability has however long been secondary when compared to
324 the scientific attention focused on providing local/regional reconstructions (Gunnarson et al.,
325 2011; Esper et al., 2012; McCarroll et al., 2013; Linderholm et al., 2014) and methodologies
326 (Björklund et al., 2012; 2014) to study temperature variability over the last several millennia.
327 Much of the tree-ring research at moisture-limited sites have until recently been limited to a
328 handful of exploratory papers (Helama and Lindholm, 2003; Linderholm et al., 2004; Jönsson
329 and Nilsson, 2009; Drobyshev et al., 2011; Seftigen et al., 2013) that generally develop one or
330 few chronologies to provide local precipitation/drought histories. These studies, together with
331 a steadily growing collection of high-latitude moisture sensitive tree-ring records (e.g.,
332 Seftigen et al., 2015), now serves as a basis for new possibilities to expand the detail and
333 accuracy with which the history of Northern European moisture conditions can be described.
334 A recent milestone in the field include the development of the “Old World Drought Atlas”
335 (“OWDA”, Cook et al., 2015), a set of tree-ring reconstructed year-to-year maps that provide
336 temporal *and* spatial details of droughts and wetness in the last millennium across Europe,

337 including Scandinavia. The OWDA has been used to elucidate hydroclimatic blueprints of the
338 Medieval Climate Anomaly (MCA, ~1000-1200 CE). Aligning with prior findings (Helama et
339 al., 2009), the atlas reveals the occurrence of so-called megadroughts in large portions of
340 continental north-central Europe and southern Scandinavia during the MCA period.
341 Interestingly, MCA and other “Old World” droughts seem to coincide with the timing of
342 some severe and persistent droughts documented in the climate history of North America.
343 While this suggests the presence of some common driving mechanisms across the North
344 Atlantic, being possibly related to variations in the Atlantic Ocean SST or/and the North
345 Atlantic Oscillation (Feng et al., 2011; Oglesby et al., 2012), the cause of these megadroughts
346 remains to be an open question.

347 While the proxy reconstructions undoubtedly play a pivotal role in unraveling
348 statistical qualities of past climate, they are, alone, not able to provide a comprehensive view
349 of the underlying physics governing the climate system. The forced-transient simulations over
350 the last millennium from fully coupled general circulation models (GCMs) (Taylor et al.,
351 2012) therefore offer an important complementary approach to the empirical analyses of
352 proxy estimates. Paleoclimate reconstructions provide an observational basis that spans
353 beyond current climate conditions that were used in developing and tuning such numerical
354 models, thus allowing for out-of-sample evaluations of the models’ predictive power. The
355 models, on the other hand, can be used to explore the dynamics that have driven climate
356 variability in the past.

357 This paper builds on previous tree-ring analyses (Seftigen et al., 2014; 2015) and
358 aims at employing a paleoclimate-data model comparison framework to further explore the
359 drivers and dynamics of drought/pluvials across Northern Europe. We analyze an ensemble of
360 six state-of-the-art GCMs from the Past Model Intercomparison Phase 3 (Schmidt et al., 2011
361 - PMIP3) and the Coupled Model Intercomparison Phase 5 (Taylor et al., 2012 - CMIP5) and
362 compare them to a new regional tree-ring-based proxy reconstruction of drought and wetness,
363 spanning the last millennium of the Common Era (CE). A combined data approach is used to
364 (1) evaluate to what extent the GCMs are capable in reproducing the key features of the
365 paleoclimate record, and (2) to estimate the role of external forcing versus internal variability
366 in driving the hydroclimatic changes regionally. **The relative contribution of changes in
367 rainfall and surface temperature at inter-annual and decadal/longer time-scales to regional
368 hydroclimate patterns is also briefly explored,** and the ability of the CMIP5/PMIP3 models to
369 simulate the mechanisms by which the regional hydroclimate is constrained by these two
370 variables are evaluated. The collective proxy-model data assessment will help to increase our

371 understanding of decadal/longer climate dynamics in regions and to evaluate the ability of the
372 state-of-the-art GCMs to simulate realistic future hydroclimatology regionally and across a
373 variety of different timescales.

374 The paper is structured as follows. Sect. 2 reviews the methods and describes the
375 paleoclimate and CMIP5/PMIP3 datasets. Subsequent analyses concentrates on comparing the
376 GCM simulations with the proxy based hydroclimate reconstructions (sect. 3), and delineating
377 the role of external (sect. 4) and internal (sect. 5) sources of variability over the last
378 millennium. The principal results and the implication of this study are discussed in sect. 6.

379 **2. Data and methods**

380 **2.1 CMIP5/PMIP3 simulations**

381 Simulations with six models (CESM1, CCSM4, IPSL-CM5A-LR, MIROC-ESM, MPI-ESM-
382 P, BCC-CSM1-1) contributing to the Coupled and Paleo Model Intercomparison Projects
383 Phases (CMIP3/PMIP3) (Schmidt et al., 2011; Taylor et al., 2012) have been used (Table I).
384 The analyses were restricted to models that have available complete monthly precipitation and
385 temperature variables spanning the last millennium (850-1849 CE) through historical (1850-
386 2005 CE) time intervals. The six millennium simulations were forced with reconstructed
387 solar, volcanic, greenhouse gas (GHG) and aerosol forcing, and partly land use changes,
388 whereas the historical simulations included natural and anthropogenic forcing (Schmidt et al.,
389 2011; Taylor et al., 2012). Except for CESM1, the analyses were limited to the first r1i1p1
390 ensemble member. Supplementary information (sect. S1, Fig. S1) provide an evaluation of six
391 selected model rainfall and temperature simulations against instrumental reference data
392 focusing on the northern European sector.

393 **2.2. Proxy data**

394 The use of annually resolved tree-ring series in the study of past hydroclimate variations has
395 traditionally been confined to lower-latitude arid and semi-arid region, with only a few
396 exceptions for the northern European sector. This is because the influence of moisture on tree-
397 growth generally decreases and is successively replaced by sensitivity to warm-season
398 temperature towards northern, cooler and wetter environment. Nevertheless, a growing body
399 of research (e.g., Helama and Lindholm, 2003; Wilson et al., 2012; Seftigen et al., 2013) has
400 established the potential to develop moisture-sensitive tree-ring chronologies in high-latitude
401 environments if a careful selection of species and sites is made. Building upon these findings,

402 we here analyse an existing network (Seftigen et al., 2014; 2015) of 25 *Pinus sylvestris* L.
403 tree-ring width chronologies from across a number of dry sites in southern Scandinavia (Fig.
404 1). The collected trees have typically been growing on well-drained soils or steep south-facing
405 slopes with warm and sunny exposure. Thus low soil moisture availability during the growing
406 season has been shown to be the most common growth-limiting factor in the tree-ring network
407 (Fig. S3 and S6).

408 The start dates of the chronologies varied across the collection, ranging from 532 to
409 1790 CE (Table II). All chronologies extended at least to year 1995. In order to reduce the
410 risk of natural/anthropogenic disturbance signal from inflicting non-climate noise upon the
411 reconstruction, the tree-ring data has been standardized in previous research (Seftigen et al.,
412 2014) by using a flexible “data-adaptive” method of standardization (Cook et al., 1995). This
413 has limited the degree to which longer-timescale climate information can be extracted.
414 Therefore, rather than using the already available hydroclimate reconstruction provided in
415 Seftigen et al. (2014), we have here re-processed the TRW collection with the newest signal-
416 free (SF) method of standardization (Melvin and Briffa, 2008), which has the capacity of
417 preserving long-term variability due to climate changes. The standardization was performed
418 with the ARSTAN software (Cook and Krusic, 2005). Chronologies combining living and
419 historical/subfossil material were standardized with a regional curve standardization (RCS)
420 approach (Briffa et al., 1992), applying a single RCS curve without any pith-offset
421 adjustments to detrend all series. To avoid spurious growth trends in the resulting RCS
422 chronologies stemming from a modern sample bias (Briffa and Melvin, 2011), tree-ring
423 datasets based only on living trees were standardized using the SF method in combination
424 with an age-dependent smoothing spline applied individually to each series. Prior to the
425 standardization, the modern chronology data were high-pass filtered and subsequently
426 grouped by means of a S-mode principal component analysis over the common interval (1792
427 – 1996 CE). The resulting eigenvector loadings are provided in supplemental material (Fig.
428 S2) and describe the major modes of high-frequency variability within the multiple modern
429 chronologies composing the dataset. The subdivision of the chronologies essentially identified
430 an east-west pattern, broadly corresponding to sub-regional differences in topography and
431 climate across the study domain. This suggested that the sub-regional tree-growth coherence
432 at high frequencies was driven by climate. Hence, it would be rational to expect a common,
433 climatically induced, growth variability also at the medium-frequency time scales, while any
434 disparities in the sub-regional tree-growth signal are likely mostly non-climatic in origin (i.e.
435 local site management practices, stand dynamics or other ‘random’ site-specific disturbances).

436 Therefore, in order to remove or minimize undesirable non-climatic noise upon our dataset,
437 modern tree-ring series were first merged group-wise as identified by the first four principal
438 components and subsequently detrended as four separate ‘batches’ using the SF method. The
439 standard version of the resulting tree-growth indices were subsequently separated and
440 averaged for each site to produce individual site chronologies. This procedure enabled us to
441 retain any shared, sub-regional, growth-forcing signal while removing site-specific medium-
442 to high-frequency noise.

443 Final data were adjusted to reduce the variance bias stemming from varying sample
444 size through time (Frank et al., 2006). The resulting chronologies were truncated where the
445 Expressed Population Signal (EPS) (Wigley et al., 1984) dropped below the 0.85 threshold,
446 or, in case of the longer chronologies, at year 1000 CE. The median segment length (MSL) of
447 all the chronologies (Table II) ranged between 74 and 357 years, and the median MSL across
448 all sites was 197 years. Although a precise quantification of returned frequency variance in
449 the final SF detrended tree-ring chronologies was not straightforward, the median MSL
450 suggested that it should be possible to use the network to reconstruct climate variability at
451 time scales up to ~200 years.

452 **2.3. Regional hydroclimatology**

453 The CMIP5/PMIP3 inter-model spread in spatial resolution and sophistication of soil
454 moisture schemes makes meaningful inter-model comparison difficult. To bypass some of
455 these challenges, the Standardized Precipitation Evapotranspiration Index (SPEI) (Vicente-
456 Serrano et al., 2013) was used to characterize the regional hydroclimatology across the study
457 domain. The SPEI, a commonly used metric of soil moisture balance, has successfully been
458 used as a target variable in several prior tree-ring reconstructions (e.g., Seftigen et al., 2014;
459 2015). The index is not a state variable but rather an offline metric of the surface moisture
460 balance that can be consistently derived across models and therefore provide standard
461 measure of hydroclimatic variability across GCMs. The computation of the index is based on
462 normalized monthly climatic water balance, i.e. cumulative precipitation minus potential
463 evapotranspiration (PET), summed over multiple time scales and computed as standard
464 deviations with respect to long-term mean (Vicente-Serrano et al., 2010). The PET was here
465 estimated with the Thornthwaite approach (Thornthwaite, 1948). The method requires surface
466 temperature and latitude data only, and has therefore frequently been used for PET
467 computations over the historical period. Moreover, the choice of methods is motivated by the
468 larger confidence that is placed on GCM simulations of temperature compared to other

469 variables (vapor pressure, wind speed, net radiation, etc.) that are required for more physically
470 based parameterizations of PET. At each grid point, model SPEI were derived from estimated
471 PET and simulated rainfall over the past1000 and historical periods and then standardized
472 against the 1901-2005 normalization period using the SPEI R package version 1.6 (Vicente-
473 Serrano et al., 2010).

474 The proxy dataset was generated by a point-by-point regression (PPR) methodology
475 that was applied to the TRW network to produce a SPEI reconstruction spanning the past
476 millennium. The climate field reconstruction method is based on principal component
477 regression procedure using the TRW chronologies as potential predictors to develop a set of
478 nested multivariate stepwise regression models (see Cook et al., 1999 for details). Here we
479 employed the same calibration/validation scheme, predictor selection and pre-processing steps
480 as previously described in Seftigen et al. (2015). We performed a full period calibration over
481 the 1901-1995 period of TRW/climate data overlap. A conventional split period
482 calibration/validation procedure was additionally performed for an independent validation of
483 the SPEI estimate, by splitting the full calibration period into two periods of roughly equal
484 length (1901-1948 and 1949-1995 periods) and computing/comparing validation metrics over
485 both periods. Each nest was centered and scaled to have the same mean and variance as the
486 observational data in the calibration period. The instrumental SPEI target field for the
487 reconstruction was computed from the CRU TS 3.22 (Harris et al., 2014) 0.5° latitude x 0.5°
488 longitude gridded rainfall and temperature datasets over the southern portion of Scandinavia
489 (55° - 65° N and 5° - 30° E) (Fig. 1), using the same conventions as described above. Simple
490 correlation analysis conclusively demonstrated a short-term early summer moisture sensitivity
491 of the TRW records over most of the study domain (Fig. S3). Based on these findings, we
492 selected June SPEI, aggregated over a 2-month time scale, as the target season data for the
493 reconstruction. A final regional time series was averaged from grid points where the
494 calibration regression models explained at least 20% of instrumental variance and the
495 reduction of error (RE) and coefficient of efficiency (CE) (National Research Council, 2006)
496 verifications metrics exceeded the generally accepted threshold value of zero across all nests
497 (N = 521 grid points). The mean tree-ring hydroclimate reconstruction (henceforth ScandH17)
498 and the corresponding instrumental target dataset are shown in Fig. 1, and a validation of the
499 reconstruction against 20th century instrumental data that have been withheld from the
500 calibration is provided in supplementary materials (Fig. S4). Results are variable depending
501 on the calibration/validation period used; the validation/calibration statistics are generally
502 stronger for the 1901-1948 period and substantially weaker for the 1949-1995 period. The

503 most recent and well-replicated nests (mid-1600s to present) are generally explaining the
504 greatest amount of instrumental variance ($R^2 > 40\%$ for the majority of the grid points). A
505 loss of grid cells with declining proxy availability and a drop in reconstruction skill is
506 occurring prior to the late-1400s and subsequently in the 1200s. Point-wise correlation with
507 gridded instrumental SPEI dataset shows that ScandH17 is representative for a larger area in
508 southern and central Scandinavia with a correlation ‘hot spot’ exceeding 0.6 (Fig. 1).

509 **2.4. Analyses**

510 The new proxy-based reconstruction was used to assess the temporal evolution of droughts
511 and pluvials over the last millennium and to elucidate the mechanisms that govern
512 hydroclimate changes in the northern European sector ranging from interannual to
513 multidecadal time scales. We briefly analyze the relative role of temperature (which
514 modulates potential evapotranspiration) and precipitation (which supplies moisture) in
515 regional hydroclimate variability (sect. 5). We use the last-millennium and historical
516 CMIP5/PMIP3 simulations of temperature and precipitation. As there are no independent,
517 annually resolved, proxy reconstructions of rainfall variability currently available for the
518 region, we only included temperature estimates in the analyses of ScandH17. For this
519 purpose, the previously published Linderholm et al. (2014) (hereafter ScandT14) summer
520 temperature reconstruction was used. The two reconstructions ScandH17 and ScandT14 share
521 no common predictors and are thus fully independent, which ensures that any circular
522 statement in the comparison can be ruled out. The ScandT14 record is based on tree-ring
523 maximum density (MXD) and blue intensity data from central-northern Scandinavia and is in
524 terms of signal strength and preserved multi-centennial scale variability one of the best
525 temperature reconstructions currently available for the region.

526 Furthermore, we extended our analyses to the model domain using the methodology
527 of paleoclimate data-model comparison. There were three main components to the combined
528 approach. Firstly, we evaluated the consistency in various datasets and assessed whether the
529 CMIP5/PMIP3 simulations have similar statistical properties as the reconstruction (sect. 3).
530 Spectral and spectral coherency analyses were performed in two ways. The first is the multi-
531 taper approach (Thomson, 1982) based on 4 tapers, where a Monte-Carlo procedure is used to
532 estimate phase 95% confidence limits. We also used the wavelet cohere analyses available in
533 the Grinsted et al. (2004) MATLAB package to assess the frequency dependent relationships
534 and phasing between various datasets.

535 Secondly, we used the Superposed Epoch Analysis (SEA) (Haurwitz and Brier,
536 1981) to evaluate the influence of volcanic aerosol forcing on hydroclimate, temperature and
537 precipitation of the Scandinavian region at inter-annual time scales (sect. 4). For the last
538 millennium, monthly mean volcanic forcing series were obtained from three different sources:
539 Gao et al. (2008), Crowley and Unterman (2013) and Sigl et al. (2015) datasets. We note that
540 the former two forcings have been used as the boundary conditions for the last millennium
541 CMIP5/PMIP3 simulations. The length of the proxy and model data allowed us to include sets
542 of the 20 largest eruptions since 1100 CE (Table III) from the annual forcing series to assess
543 the mean response. For each series and eruption, anomalies for ten post-eruption years were
544 computed relative to a five-year pre-eruption mean. The confidence intervals around the
545 composite responses were determined using a Monte Carlo block resampling ($N = 10\,000$) of
546 the actual event year windows (see Adams et al., 2003 for details).

547 Thirdly, we evaluated the skill of the models to represent the dynamics that drive the
548 variability in hydroclimate of the Scandinavian region by establishing a link between
549 simulated and reconstructed SPEI series and fields of mean sea level pressure (MSLP) over
550 the Atlantic-European sector (sect. 5). Grid point correlations were computed to assess the
551 spatial features and the strength of the teleconnections patterns over the modern era (1950-
552 2005 CE). The analysis was also extended over the last millennium (1000-1849 CE) to
553 investigate the nature of teleconnection stability without the influence of anthropogenic
554 forcing. The gridded monthly instrumental HadSLP2 dataset spanning 1850-present (Allan
555 and Ansell, 2006) was used for comparison with observed and proxy-based estimates of
556 hydroclimate.

557 **3. Modeled and reconstructed hydroclimate series**

558 The regional warm season hydroclimate variability averaged across the six CMIP5/PMIP3
559 models together with the new ScandH17 proxy reconstruction over the last millennium are
560 shown in Fig. 2a-b. Individual model SPEI time series are displayed in Fig. 2c-h. All data
561 have been normalized and centred over the common interval from 1000 to 1995 CE, since this
562 first joint proxy-model comparison focuses on the common relative changes rather than on the
563 magnitude and the absolute values. A simple visual comparison reveals that the models and
564 the reconstruction have generally little agreement in the variance structure and trends. The
565 reconstruction is dominated by a large decadal-to-multidecadal variability while the
566 multimodel mean is relatively flat at these time scales. There are some common features in
567 some of the GCMs and the proxy datasets though (Fig. 2c-h), e.g., the drying in the 19th

568 century, but these are rare when the full millennium is considered and are likely occurring by
569 chance. The historical interval in the proxy record is characterized by a drought in the mid-
570 1800s and a gradual increase in wetness over the 20th century, while, with the exception of
571 short dry episode in the early-1900s, there is no long-term trend in the multimodel mean over
572 the modern era.

573 The very low correlation at inter-annual time scales is to be expected, as the internal
574 variations in the various records represent different realizations of the climate system, which
575 is to a very large extent chaotic at that time scale. The response of each ensemble member to a
576 strong external forcing applied to the model would nevertheless ideally agree (i.e. external
577 punctual perturbations such as volcanic eruptions could induce a coherent short-term
578 response, see sect. 4). Averaging across models or over multiple ensemble members will
579 reduce the contribution from stochastic variability so that the remaining signal can come
580 closer to the model response to external forcing. The comparison between ScandH17 and the
581 multimodel assemble mean reveal, however, no statistically significant agreement between
582 the series, neither on the interannual nor on decadal timescales, suggesting that the simulated
583 hydroclimate changes are not strongly tied to exogenous forcing. Moreover, we found no
584 statistically significant correlation between the different ensemble members in the same
585 model (CESM1) (Fig. 2c), which is the only model providing multiple ensemble members
586 (the only difference among these being the air temperature at the start of each ensemble
587 member (Otto-Bliesner et al., 2016) over the historical and past millennium intervals). The
588 poor overlap between CESM1 ensemble members as well as the individual GCM simulations
589 over the past millennium (despite the use of largely similar forcing series to drive the
590 simulations) is indicative of a larger contribution from internal variability on simulated
591 drought/pluvial occurrence than from changes in exogenous forcing.

592 We compare the spectral properties of the six individual CMIP5/PMIP3 models to
593 the ScandH17 reconstruction and observational data, which allows for a general evaluation of
594 potential frequency biases. Results indicate that the underlying spectrum of reconstructed
595 hydroclimate variability is significantly redder on decadal-centennial timescales than
596 indicated by the simulated SPEI (Fig. 3a and 3d), as has previously been noted (Ault et al.,
597 2012; Ault et al., 2013). In contrast, more hydroclimate variance is concentrated on
598 interannual timescales in the CMIP5/PMIP3 archive than in ScandH17 reconstruction. At
599 frequency bands < 8 years, the power spectral range of most models is systematically above
600 the confidence interval of ScandH17. We also consider the agreement between simulated,
601 reconstructed (ScandT14) and instrumental temperature data in terms of their spectral

602 properties (Fig. 3b). Although the degree of agreement is higher than for hydroclimatology
603 and most models lie within the reconstruction confidence bands (see also sect. S2
604 supplementary materials), there are some models that have more variance than the
605 reconstruction at periods < 10 years.

606 **4. The role of volcanic forcing**

607 Large explosive volcanic eruptions are an important natural radiative forcing mechanism at
608 timescales ranging from seasons to decades (Shindell et al., 2004; Gleckler et al., 2006). The
609 imposed perturbation on the climate system by such events will depend on the nature of the
610 eruption, the magnitude of change in the energy entering the earth's atmosphere, the
611 background climate and internal variability, latitude and season. Analysis of observational
612 data (Shindell et al., 2004), tree-ring records (D'Arrigo et al., 2013) and model simulations
613 (Anchukaitis et al., 2010) indicate a considerable spatial variability in the dynamical response
614 of the climate system to volcanic forcing, with some regions experience surface and
615 tropospheric cooling effects and other regions showing no significant change or even
616 warming effect. Here, we assess the magnitude and timing of Scandinavian summer
617 temperature, rainfall and hydroclimate response to short-term radiative cooling due to
618 volcanic aerosols.

619 A peak cooling is observed one year after the eruption, both in ScandT14 and in the
620 CMIP5/PMIP3 composite average, for all the three forcings considered (Fig. 4). In addition,
621 there is a significant cooling in the year of the event for the Crowley and Unterman (2013)
622 and Sigl et al. (2015) lists. ScandT14 reveal a marginally greater cooling (2.0 °C, mean of the
623 three event lists) than the model average (1.8 °C) one year after the eruption. Remarkably,
624 there is a high degree of similarity in the proxy and in the GCMs not only in terms of the
625 signal timing and the magnitude of the cooling response, but also the rate of recovery. A
626 complete recovery after the volcanic cooling is found two years after the eruption,
627 independent of the forcing list. These results are generally consistent with prior studies
628 (Fischer et al., 2007; Jones et al., 2013; McCarroll et al., 2013) highlighting the importance of
629 explosive volcanism as an external driver of Northern European temperature variability. They
630 also provide a relevant test of the model to radiation perturbations. The agreement between
631 the model simulations and proxy data demonstrates the credibility of the models.

632 Existing research on the response of high-latitude rainfall and hydroclimate to
633 volcanism is limited (in part because high resolution moisture sensitive proxy records are
634 sparse or unavailable). Fischer et al. (2007) found a weak tendency to drying conditions over

635 southern/central Scandinavia in the summer of year 0 and year 1 after the eruption.
636 Circulation changes to the surface cooling were shown to modulate the directly forced
637 response. On continental and global scales, both observational and modeling studies have
638 found a decrease in precipitation (Iles et al., 2013) and streamflow (Iles and Hegerl, 2015) in
639 response to large explosive eruptions, particularly in climatologically humid regions (Carley
640 and Gabriele, 2014). The short-term drying is caused by a reduction in incoming solar
641 radiation reaching the surface, which reduces evaporation, whilst the widespread cooling
642 stabilized the atmosphere and lowers its water holding capacity (Bala et al., 2008). Here, we
643 apply SEA on ScandH17 and simulated SPEI and precipitation to examine the influence of
644 volcanism on Scandinavian moisture availability. A statistically significant reduction in
645 simulated rainfall is observed for all event lists, ranging between the year of the event
646 (Crowley and Unterman, 2013 dataset) and up to two years (Sigl et al., 2015 dataset)
647 following the eruption. We find, however, that the precipitation signal is less consistent across
648 the six CMIP5/PMIP3 models than the cooling effect observed in the simulated temperature
649 series.

650 The SEA on SPEI time series reveals a statistically significant drying after large
651 volcanism. However, the response is more muted than the response of temperature and
652 rainfall separately. Moreover, the agreement between proxy data and the model composite
653 average is weak and there are large inconsistencies between the different forcing records.
654 ScandH17 show a progressive transition from wet conditions in the event year and preceding
655 years to dryer conditions in the consecutive years with significant dry anomalies five
656 (Crowley and Unterman, 2013 dataset) and seven years (Sigl et al., 2015; Gao et al., 2008
657 datasets) after the perturbation. For the CMIP5/PMIP3 multimodel multi-eruption average,
658 only the fifth year after the eruption (Crowley and Unterman, 2013 list) is found to be
659 significantly drier than the adjacent years.

660 The observed weak influence of volcanic forcing on the hydroclimate of the region
661 can be explained by various factors. For example, our results reveal that GCM simulated post-
662 volcanic cooling remains significant for about two years and matches the timescale of the
663 post-volcanic rainfall decrease. Since the SPEI accounts for both supply and demand changes,
664 the net effect would be such that the temperature-driven PET decrease counter a substantial
665 fraction of the precipitation-driven drying, thus producing SPEI values near neutral.
666 Furthermore, the muted response of ScandH17 may arise from autocorrelated biological
667 memory in the TRW data (Esper et al., 2015). The high year-to-year persistence may bias its
668 ability to estimate the abruptness and severity of climatic extremes caused by volcanic

669 cooling. The tree-ring MXD and the blue intensity parameters have, in contrast, been
670 suggested to be superior to TRW for recording short term climate perturbations (Wilson et al.,
671 2016), which is likely the reason why the response of ScandT14 is more immediate than that
672 of ScandH17.

673 **5. Internal sources of variability**

674 If the regional hydroclimate variability is indeed dominated by internally generated stochastic
675 components of variability (see sect. 3), atmospheric circulation changes can be the key
676 process shaping regional patterns of moisture availability. Advancing our understanding of
677 the range, stability and strength of teleconnection behavior (defined here as the correlation
678 between hydroclimate and MSLP over the Atlantic-European sector) and its coupling to
679 regional hydroclimate would provide an improved understanding of drought/pluvial dynamics
680 and associated uncertainty. In this section, we first explore major modes of atmosphere
681 variability that impact summertime northern European hydroclimatology. We also assess
682 more extensively the contribution of atmospheric processes (and possible land-atmosphere
683 interactions) by investigating the couplings between hydroclimate and arguably the two most
684 critical variables of the terrestrial climate and the hydrological cycle: precipitation and
685 temperature.

686 To determine the role of teleconnections, correlation of MSLP fields with the
687 hydroclimatic variables over the recent 50 years of the post-industrial era were computed.
688 Results are shown in Fig. 5. As expected, we find that atmospheric dynamics have a
689 significant role in climate variability in the region: a strong correlation with regional
690 hydroclimate is found when MSLP in concurrent months (i.e. May-June) is considered. The
691 results show that the proxy based and CMIP5/PMIP3 simulated dynamics are largely
692 consistent with those in the instrumental record, indicating that both the proxy and the models
693 contain to some degree realistic teleconnections. A consistent feature across the datasets is a
694 tripole structure that would favor increased moisture supply into the Scandinavian region. The
695 structure is characterized by anomalous cyclonic conditions across Scandinavia and high-
696 pressure systems extending over Iceland-Greenland and, albeit less pronounced, over
697 European Russia - Central Asia. Out of the six CMIP5/PMIP3 models, MIROC-ESM is the
698 one showing the largest discrepancy with the major spatial features of the observed
699 correlation map, by failing to reproduce the anti-cyclonic pattern over Iceland-Greenland.
700 Additionally, MIROC-ESM and also CCSM4 show a meridional and zonal shift of the
701 European Russia - Central Asia high-pressure structure towards the Mediterranean region.

702 Atmospheric circulation has been identified as key contributor to recent changes in
703 the climate of Europe in both summer and winter (van Oldenborgh and Van Ulden, 2003;
704 Jones and Lister, 2009). To assess the stationarity of observed MSLP patterns, the analysis
705 was repeated for the pre-industrial last millennium (1000-1849 CE) period (Fig. 6). The
706 exercise was restricted to five GCMs for which simulated MSLP was available for the pre-
707 industrial era (BCC-CSM1-1 was not included). The simulated dynamical relationships were
708 found to be largely stable for all five models, being consistent with observed correlations
709 patterns in the modern era. This suggests a weak influence of anthropogenic forcing on the
710 structure of the dynamical drivers of Scandinavian hydroclimate. In addition to raw data,
711 correlation analysis with 10-year low-passed data was also completed for the pre-industrial
712 period with the purpose to elucidate the drivers of multidecadal hydroclimate variability. We
713 find similar, yet weaker, correlation patterns as compared to the high-frequency variations
714 (results not shown).

715 Precipitation and temperature are the two key variables of the hydrological cycle.
716 Assessing the relative contribution of these two variables to the surface moisture balance
717 across various timescales, and the mechanisms that control and modulate it, is therefore of
718 great interest to the study of regional processes on surface energy and water budgets. While
719 past studies have investigated the relationship between temperature, moisture supply and
720 drought in various regions on daily, seasonal and interannual timescales (Adler et al., 2008;
721 Berg et al., 2015; Trenberth, 2011; Madden and Williams, 1978), the nature of concurrent
722 multidecadal/ long-term relationship is still far from being clear. A joint analyses of the new
723 hydroclimate reconstruction with the recently published Linderholm et al. (2014- ScandT14)
724 fully independent warm-season temperature record for Scandinavia is provided in Figs. 7 and
725 8, in conjunction with the CMIP5/PMIP3 simulations of temperature, rainfall and SPEI. On
726 interannual timescales, five out of six GCMs show a significant ($p < 0.05$) negative
727 association between simulated interannual temperature and rainfall, with correlation
728 coefficients ranging between $r = -0.12$ and -0.29 (1000-2005 CE period). Moreover, all model
729 show a strong negative (positive) correlation between temperature (precipitation) and SPEI in
730 the last millennium, ranging between $r = -0.63$ and -0.80 ($r = 0.61$ and 0.84). Extending the
731 analysis to the instrumental data, we find that the regional year-to-year variability in
732 hydroclimate is more closely organized around changes in precipitation than changes in
733 temperature (Fig. S5). In southern Scandinavia, weak negative correlations appear between
734 temperature and rainfall (Fig. S5a), and temperature and SPEI (Fig. S5b). Over northern
735 Scandinavia, the interannual correlations are not significant.

736 Turning to the tree-ring records, we find no significant relationship between
737 ScandH17 and ScandT14 reconstructions on a year-to-year basis ($r = 0.01$ and $p = 0.8$ on first
738 difference data, 1100-1995 CE period). The considerable distance separating the sampling
739 sites of each tree-ring collection, and the fact that summer precipitation occurrence often
740 depends on local processes and moisture fluxes could explain the lack of a shared annual
741 signal. Notably, however, we find that the two reconstructions are mostly in phase on decadal
742 and longer timescales ($r = 0.30$ and $p < 0.001$ on loess-smoothed data, 1100-1995 CE period)
743 (Fig. 7), suggesting that the low-frequency temperature and hydroclimate variability is more
744 spatially coherent. These results are corroborated by the cross-wavelet coherency analysis
745 (Fig. 8a), revealing that the ScandH17 and ScandT14 reconstructions share significant ($p <$
746 0.05) in phase variance in multidecadal frequency throughout most of the last millennium.
747 The coupling seems to arise from overlap in shared frequencies at wavelengths longer than \sim
748 50 years (c.f. Fig. 3). Interestingly, we find that the paleoclimatic evidence and the
749 CMIP5/PMIP3 models portray a considerably different response of hydroclimate in
750 Scandinavia to long-term temperature changes. While the proxy time series suggests that
751 prolonged wet periods generally coincide with elevated temperatures, the majority of the
752 CMIP5/PMIP3 models indicate that warm decades should have been dryer (Fig. 8b – h and
753 Fig. S9).

754 Instrumental and paleoclimate evidence collectively suggest a time-dependent shift
755 of the relationship between regional temperature and hydroclimate, which in turn implies that
756 different mechanisms governing the climate system might be operating at high (interannual)
757 and low (decadal/longer) frequencies, respectively. The previously discussed strong link
758 between inter-annual regional hydroclimate variability and atmospheric pressure patterns
759 indicates that atmospheric dynamics is likely a dominant driver of hydroclimate in the
760 northern European sector on interannual basis. The inverse covariability between warm-
761 season temperature and moisture supply, which is revealed by the instrumental record, may
762 arise from synoptic-scale correspondence between reduced cloud cover/rainfall and increased
763 incoming shortwave radiation warming the surface during clear sky conditions. In addition,
764 soil moisture exert a strong influence on the allocation of available energy between latent and
765 sensible heating, especially in the warm-season (Seneviratne et al., 2010). Reduced soil
766 moisture, for example, is associated with reduced latent heat flux and thus increased sensible
767 heating and higher air temperatures near the surface. Resulting positive feedbacks of a
768 modified surface heat flux partitioning on cloud cover and radiation (Gentine et al., 2013) and

769 large-scale circulation (Haarsma et al., 2009) could further strengthen the influence of rainfall
770 variability on the thermal climate.

771 The positive association between temperature and SPEI that is found in the proxy
772 records on decadal-to-multidecadal timescales could imply that the long-term regional
773 hydroclimate variability is more sensitive to changes in moisture supply (precipitation) rather
774 than to increased evaporative demand due to warming. It may also suggest that the regional
775 moisture balance might be favored by the Clausius-Clapeyron relation (Allen and Ingram,
776 2002), prescribing an increase in rainfall and intensity of the hydrological cycle during
777 warmer periods in the past millennium. This is generally referred to as ‘wet-get-wetter’/‘dry-
778 get-drier’ mechanism and is attributed to thermodynamics processes (Held and Soden, 2006).
779 In the absence of changes in atmospheric circulation, changes in net moisture supply with
780 warming are related to change in moisture content of the atmosphere. It presupposes that
781 existing circulations will transport more moisture into mesic regions of the globe (e.g., tropics
782 and the mid- to latitudes of Northern Hemisphere), whilst dry regions (e.g., subtropics) will
783 get even dryer, with the fractional change determined by Clausius-Clapeyron relation. In
784 contrast to the proxy records, the model composite average reveals a twentieth-century
785 temperature and rainfall increase yet little change in hydroclimate (Fig. 7b). The multimodel
786 assessment implies that natural variability plays only a subsidiary role in recent changes and
787 that forcing from anthropogenic greenhouse gases (GHG) may have played a more important
788 role (as previously discussed, the effect of GHG-forcing on interannual teleconnection
789 patterns in the modern era seems to be weak). Moreover, the absence of any significant trend
790 in simulated SPEI series indicates that the gains in moisture from increased precipitation are
791 large enough to compensate for any GHG-induced increase in PET in the post-industrial
792 period.

793 **6. Summary and discussion**

794 This study presents the first comprehensive assessment of past variability and trends in
795 hydroclimate of northern European sector over the last millennium of the Common Era along
796 with interrelated variables: precipitation, which supplies moisture, and temperature, which
797 modulates evapotranspiration. A combined approach comparing observational (both
798 instrumental and proxy based) and model-based results is used for evaluation of simulated
799 and real-world interannual-to-centennial climate variability and the underlying physics
800 governing the climate system. A number of important findings emerge from the collective
801 comparison:

802 [1] Models and proxy data are found to broadly agree on the modes of atmospheric variability
803 (sect. 5) that produces droughts and pluvials in Scandinavia. Despite these dynamical
804 similarities, large discrepancies between model simulations and the proxy reconstruction are
805 shown to exist. The droughts and pluvials in the forced simulation are not temporally
806 synchronous with those in the proxy record, nor do the GCM spectra agree with the proxy
807 spectra on the amount of variance present on short and long timescales (sect. 3).

808 [2] The proxy data and the CMIP5/PMIP3 models reveal different effects of long-term
809 temperature changes on summer hydroclimate in Scandinavia. According to the GCMs,
810 prolonged droughts generally coincide with elevated temperatures. The proxy evidence, on
811 the other hand, suggests that warm decades in the last millennium also tend to be wet decades.
812 Although the precise reason for the model-proxy mismatch remains to be unraveled, our
813 results suggests that spectral inconsistencies among the model and proxy datasets could be
814 one possible explanation for the mismatch.

815 [3] There are considerable disagreements among hydroclimate features shown by the
816 CMIP5/PMIP3 simulations (despite the use of largely similar forcing series) (sect. 3).
817 Together, these results point to the possibilities of dominant influence of stochastic processes
818 for the regional hydroclimate and/or deficiencies in the models to realistically represent
819 relevant processes in reality.

820 Most notably we find clear inconsistencies between the paleoclimate record and the
821 model spectra. At multidecadal/longer timescale there is more variability in the proxy data
822 than in the models. In contrast, the dominance of GCM simulated interannual components of
823 variability is not reflected in the proxy record. It is difficult to determine explicitly whether it
824 is an external forcing or internal sources that drive the decadal and longer variance in the
825 proxy reconstruction. Prior studies have highlighted the importance of external influences on
826 regional climate variability at different timescales (e.g., Gleckler et al., 2006; Thiéblemont et
827 al., 2015; Sigl et al., 2015). Although we find a short term response of regional hydroclimate
828 to volcanic perturbations (sect. 4), multi-year anomalies in the proxy reconstruction do,
829 however, not appear to correspond well with the epochs following the large volcanic
830 eruptions (e.g., in the 1250s, 1450s and 1810s) used to force the models. Thus we cannot rule
831 out that the variability in the reconstruction largely arise from internal sources of variation.
832 Consequently, if the proxy-inferred decadal-to-multidecadal variability is accurate and if the
833 variability is indeed largely unforced, then its magnitude is well beyond what any of the
834 current generation global climate models are able to produce in the region. Underestimation
835 of redness in the models on multidecadal/longer timescales, suggests the GCMs might be

836 lacking/underestimating processes important to the variability at these timescales. There are a
837 number of recognized limitations relating to the dynamics that are relevant to the climatology
838 of the North Atlantic-European sectors. One such example is that models have generally been
839 unable to simulate low-frequency variability in the North Atlantic Oscillation (Osborn, 2004).
840 They have also been shown to underestimate the periodicity of the Atlantic Multidecadal
841 Oscillation (Kavvada et al., 2013), which has implications for the associated hydroclimate
842 impact on neighboring continents (Coats et al., 2015). If, on the other hand, the proxy
843 estimated multidecadal/longer variability in the last millennium is forced by exogenous
844 mechanisms, then either 1) it is a forcing component that is largely missing in the
845 CMIP5/PMIP3 models, alternatively, 2) it is a forcing component that generates a different
846 long-term response in the models compared to the “proxy view” of regional
847 hydroclimatology.

848 It is not possible to pinpoint which part of the disagreement between models and the
849 proxy comes from uncertainties in the tree-ring reconstruction, deficiencies in the forcing
850 series used to drive the models, or from deficiencies in the model. Our analyses have included
851 precipitation simulation – a challenging variable for GCMs to simulate accurately. The coarse
852 spatial resolution of the models gives only an approximate representation of the topographic
853 features, which are important for regional hydroclimate. Another possibility is that the scale
854 of the GCMs is unrepresentative of the point estimate provided by the ScandH17
855 reconstruction. On the other hand, the mismatch between grid box and point estimates is
856 expected to reduce at longer timescales (Jones et al., 1997). There are also limitations of the
857 tree-ring proxy and uncertainties in the interpretation of the data that cannot be ignored. Tree-
858 rings and other biological archives may integrate climate conditions over multiple years
859 (Zhang et al., 2015), which could potentially overestimating the ratio of low to high frequency
860 variability (Franke et al., 2013). While we have been able to establish that prevailing summer
861 moisture availability has been the main growth limitation of trees in the ScandH17 network
862 on an interannual basis over the twentieth century (Figs. S3 and S6), we cannot verify the
863 drought-tree growth model in the pre-instrumental era or across longer spectrum of
864 variability. We are not able to rule out that there might have been climatic regimes in the past
865 that would have caused dynamical shift in the tree growth response to climate, and potentially
866 have called into question the uniformitarian paradigm traditionally applied in the field of
867 dendroclimatology. These non-stationaries may include frequency dependent sensitivity of the
868 proxy system to climate. While we are able to show that the year-to-year variability of growth
869 is dominated by a moisture signal, the impact of growing season temperature on lower

870 frequency variations has yet to be established. In addition to these issues, there are also risks
871 that less well know dynamics outside the climate system may introduce variability into the
872 records at decadal/longer timescales. Advances in the mechanistic understanding of the
873 various proxies and the processes through which they record environmental change, e.g.,
874 through development and refinement of process-based forward models (Tolwinski-Ward et
875 al., 2011), is currently an emerging priority in the field.

876 The discrepancies in CMIP5/PMIP3 simulated and proxy reconstructed hydroclimate
877 variability in the last millennium is an issue that must be addressed when assessing
878 projections of future hydroclimate change. The lack of adequate understanding for
879 mechanisms linking temperature and moisture supply on longer timescales has important
880 implication for future projections. Weak multidecadal variability in models also implies that
881 inference about future persistent droughts and pluvials based on the latest generation global
882 climate models will likely underestimate the true risk of these events. Reconciliations for the
883 apparent proxy – model mismatch will require efforts from the proxy, modeling and statistics
884 groups, including additional proxy records and refined model simulations of hydroclimate
885 variability in the last millennium, together with the development of alternative approaches for
886 joint proxy-model assessments. Having here provided a first comparison of reconstructed and
887 simulated hydroclimate for Scandinavia, our future efforts will include adaptations of the data
888 assimilation approach to paleoclimate reconstruction. Such efforts hold promise for reducing
889 the uncertainties associated with model physics, external forcings, and internal climate
890 variability, and ultimately help to refine our view of past and future hydroclimate changes.

891 **Data availability**

892 The raw tree-ring data can be downloaded from the International Tree-Ring Data Bank
893 (<http://www.ncdc.noaa.gov/paleo/treering.html>) and the SAIMA Tree-Ring Data Bank
894 (<http://lustiag.pp.fi/Saima/dendrotieto.htm>) (Table II). The CMIP5/PMIP3 climate model
895 output can be obtained though the Earth System Grid - Center for Enabling Technologies
896 (ESG-CET) portal (<http://pcmdi9.llnl.gov/>). The ScandT14 temperature reconstruction is
897 archived through the NOAA paleoclimate database (citation added on publication). The
898 ScandH17 reconstruction and standardized tree-ring chronologies are provided in the
899 supporting information.

900 **Acknowledgments**

901 K. Seftigen was supported by the FORMAS mobility starting grant for young researchers
902 (grant # 2014-723). H. Goosse is senior research associate with the FRS/FNRS, Belgium. The
903 authors wish to acknowledge the World Climate Research Programme's Working Group on
904 Coupled Modelling, which is responsible for CMIP, and to thank the climate modeling groups
905 (listed in Table I of this paper) for producing and making available their model output. For
906 CMIP the U.S. Department of Energy's Program for Climate Model Diagnosis and
907 Intercomparison provides coordinating support and led development of software
908 infrastructure in partnership with the Global Organization for Earth System Science Portals.
909 The authors also wish to acknowledge the researchers who have produced and made their
910 tree-ring chronologies available.

911 **References**

- 912 Adams, B. J., Mann, M. E., and Ammann, C. M.: Proxy evidence for an El Nino-like response to
913 volcanic forcing, *Nature*, 426, 274-278, 2003.
- 914 Adler, R. F., Gu, G., Wang, J.-J., Huffman, G. J., Curtis, S., and Bolvin, D.: Relationships between
915 global precipitation and surface temperature on interannual and longer timescales (1979–2006),
916 *Journal of Geophysical Research*, 113, 10.1029/2008jd010536, 2008.
- 917 Allan, R., and Ansell, T.: A New Globally Complete Monthly Historical Gridded Mean Sea Level
918 Pressure Dataset (HadSLP2): 1850–2004, *Journal of Climate*, 19, 5816-5842, 10.1175/jcli3937.1,
919 2006.
- 920 Allen, M. R., and Ingram, W. J.: Constraints on future changes in climate and the hydrologic cycle,
921 *Nature*, 419, 224-232, 2002.
- 922 Anchukaitis, K. J., Buckley, B. M., Cook, E. R., Cook, B. I., D'Arrigo, R. D., and Ammann, C. M.:
923 Influence of volcanic eruptions on the climate of the Asian monsoon region, *Geophysical Research*
924 *Letters*, 37, n/a-n/a, 10.1029/2010gl044843, 2010.
- 925 Ault, T. R., Cole, J. E., and St. George, S.: The amplitude of decadal to multidecadal variability in
926 precipitation simulated by state-of-the-art climate models, *Geophysical Research Letters*, 39, n/a-n/a,
927 10.1029/2012gl053424, 2012.
- 928 Ault, T. R., Cole, J. E., Overpeck, J. T., Pederson, G. T., St. George, S., Otto-Bliesner, B.,
929 Woodhouse, C. A., and Deser, C.: The Continuum of Hydroclimate Variability in Western North
930 America during the Last Millennium, *Journal of Climate*, 26, 5863-5878, 10.1175/jcli-d-11-00732.1,
931 2013.
- 932 Bala, G., Duffy, P. B., and Taylor, K. E.: Impact of geoengineering schemes on the global
933 hydrological cycle, *Proceedings of the National Academy of Sciences*, 105, 7664-7669,
934 10.1073/pnas.0711648105, 2008.
- 935 Berg, A., Lintner, B. R., Findell, K., Seneviratne, S. I., van den Hurk, B., Ducharne, A., Chéruey, F.,
936 Hagemann, S., Lawrence, D. M., Malyshev, S., Meier, A., and Gentine, P.: Interannual Coupling
937 between Summertime Surface Temperature and Precipitation over Land: Processes and Implications
938 for Climate Change*, *Journal of Climate*, 28, 1308-1328, 10.1175/jcli-d-14-00324.1, 2015.
- 939 Björklund, J., Gunnarson, B. E., Krusic, P. J., Grudd, H., Josefsson, T., Östlund, L., and Linderholm,
940 H. W.: Advances towards improved low-frequency tree-ring reconstructions, using an updated *Pinus*
941 *sylvestris* L. MXD network from the Scandinavian Mountains, *Theor Appl Climatol*, 10.1007/s00704-
942 012-0787-7, 2012.
- 943 Björklund, J., Gunnarson, B. E., Seftigen, K., Esper, J., and Linderholm, H. W.: Blue intensity and
944 density from northern Fennoscandian tree rings, exploring the potential to improve summer
945 temperature reconstructions with earlywood information, *Climate of the Past*, 10, 877-885,
946 10.5194/cp-10-877-2014, 2014.

947 Briffa, K. R., Jones, P. D., Bartholin, T. S., Eckstein, D., Schweingruber, F. H., Karlén, W.,
948 Zetterberg, P., and Eronen, M.: Fennoscandian summers from ad 500: temperature changes on short
949 and long timescales, *Climate Dynamics*, 7, 111-119, 10.1007/bf00211153, 1992.

950 Briffa, K. R., and Melvin, T. M.: A Closer Look at Regional Curve Standardization of Tree-Ring
951 Records: Justification of the Need, a Warning of Some Pitfalls, and Suggested Improvements in Its
952 Application, in: *Dendroclimatology: Progress and Prospects*, edited by: Hughes, M. K., Swetnam, T.
953 W., and Diaz, H. F., Springer Netherlands, Dordrecht, 113-145, 2011.

954 Carley, E. I., and Gabriele, C. H.: The global precipitation response to volcanic eruptions in the
955 CMIP5 models, *Environmental Research Letters*, 9, 104012, 2014.

956 Coats, S., Cook, B. I., Smerdon, J. E., and Seager, R.: North American Pancontinental Droughts in
957 Model Simulations of the Last Millennium*, *Journal of Climate*, 28, 2025-2043, 10.1175/jcli-d-14-
958 00634.1, 2015.

959 Cook, E. R., Briffa, K. R., Meko, D., Graybill, D. A., and Funkhouser, G.: The 'segment length curse'
960 in long tree-ring chronology development for palaeoclimatic studies, *The Holocene*, 5, 229-237, 1995.

961 Cook, E. R., Meko, D. M., Stahle, D. W., and Cleaveland, M. K.: Drought Reconstructions for the
962 Continental United States, *Journal of Climate*, 12, 1145-1162, 1999.

963 Cook, E. R., and Krusic, P. J.: Arstan, version 2005, Tree-ring labora- tory, Lamont-Doherty Earth
964 Obs., Palisades, N. Y. (Available at <http://www.ldeo.columbia.edu/trl>), 2005.

965 Cook, E. R., Seager, R., Kushnir, Y., Briffa, K. R., Büntgen, U., Frank, D., Krusic, P. J., Tegel, W.,
966 van der Schrier, G., Andreu-Hayles, L., Baillie, M., Baittinger, C., Bleicher, N., Bonde, N., Brown, D.,
967 Carrer, M., Cooper, R., Čufar, K., Dittmar, C., Esper, J., Griggs, C., Gunnarson, B., Günther, B.,
968 Gutierrez, E., Haneca, K., Helama, S., Herzig, F., Heussner, K.-U., Hofmann, J., Janda, P., Kontic, R.,
969 Köse, N., Kyncl, T., Levanič, T., Linderholm, H., Manning, S., Melvin, T. M., Miles, D., Neuwirth,
970 B., Nicolussi, K., Nola, P., Panayotov, M., Popa, I., Rothe, A., Seftigen, K., Seim, A., Svarva, H.,
971 Svoboda, M., Thun, T., Timonen, M., Touchan, R., Trotsiuk, V., Trouet, V., Walder, F., Ważny, T.,
972 Wilson, R., and Zang, C.: Old World megadroughts and pluvials during the Common Era, *Science*
973 *Advances*, 1, 10.1126/sciadv.1500561, 2015.

974 Crowley, T. J., and Unterman, M. B.: Technical details concerning development of a 1200 yr proxy
975 index for global volcanism, *Earth Syst. Sci. Data*, 5, 187-197, 10.5194/essd-5-187-2013, 2013.

976 D'Arrigo, R., Wilson, R., and Anchukaitis, K. J.: Volcanic cooling signal in tree ring temperature
977 records for the past millennium, *Journal of Geophysical Research: Atmospheres*, 118, 9000-9010,
978 10.1002/jgrd.50692, 2013.

979 Drobyshev, I., Niklasson, M., Linderholm, H. W., Seftigen, K., Hickler, T., and Eggertsson, O.:
980 Reconstruction of a regional drought index in southern Sweden since AD 1750, *The Holocene*, 21,
981 667-679, 10.1177/0959683610391312, 2011.

982 Dufresne, J. L., Foujols, M. A., Denvil, S., Caubel, A., Marti, O., Aumont, O., Balkanski, Y., Bekki,
983 S., Bellenger, H., Benshila, R., Bony, S., Bopp, L., Braconnot, P., Brockmann, P., Cadule, P., Cheruy,
984 F., Codron, F., Cozic, A., Cugnet, D., de Noblet, N., Duvel, J. P., Ethé, C., Fairhead, L., Fichefet, T.,
985 Flavoni, S., Friedlingstein, P., Grandpeix, J. Y., Guez, L., Guilyardi, E., Hauglustaine, D., Hourdin, F.,
986 Idelkadi, A., Ghattas, J., Joussaume, S., Kageyama, M., Krinner, G., Labetoulle, S., Lahellec, A.,
987 Lefebvre, M. P., Lefèvre, F., Levy, C., Li, Z. X., Lloyd, J., Lott, F., Madec, G., Mancip, M.,
988 Marchand, M., Masson, S., Meurdesoif, Y., Mignot, J., Musat, I., Parouty, S., Polcher, J., Rio, C.,
989 Schulz, M., Swingedouw, D., Szopa, S., Talandier, C., Terray, P., Viovy, N., and Vuichard, N.:
990 Climate change projections using the IPSL-CM5 Earth System Model: from CMIP3 to CMIP5,
991 *Climate Dynamics*, 40, 2123-2165, 10.1007/s00382-012-1636-1, 2013.

992 Esper, J., Frank, D. C., Timonen, M., Zorita, E., Wilson, R. J. S., Luterbacher, J., Holzkamper, S.,
993 Fischer, N., Wagner, S., Nievergelt, D., Verstege, A., and Buntgen, U.: Orbital forcing of tree-ring
994 data, *Nature Clim. Change*, 2, 862-866, 2012.

995 Esper, J., Schneider, L., Smerdon, J. E., Schöne, B. R., and Büntgen, U.: Signals and memory in tree-
996 ring width and density data, *Dendrochronologia*, 35, 62-70,
997 <http://dx.doi.org/10.1016/j.dendro.2015.07.001>, 2015.

998 Feng, S., Hu, Q., and Oglesby, R. J.: Influence of Atlantic sea surface temperatures on persistent
999 drought in North America, *Climate Dynamics*, 37, 569-586, 10.1007/s00382-010-0835-x, 2011.

1000 Fischer, E. M., Luterbacher, J., Zorita, E., Tett, S. F. B., Casty, C., and Wanner, H.: European climate
1001 response to tropical volcanic eruptions over the last half millennium, *Geophysical Research Letters*,
1002 34, n/a-n/a, 10.1029/2006GL027992, 2007.

1003 Frank, D. C., Esper, J., and Cook, E. R.: On variance adjustments in tree-ring chronology
1004 development, *Tree rings in archaeology, climatology and ecology*, TRACE, 4, 56-66, 2006.

1005 Franke, J., Frank, D., Raible, C. C., Esper, J., and Bronnimann, S.: Spectral biases in tree-ring climate
1006 proxies, *Nature Clim. Change*, 3, 360-364, 2013.

1007 Gao, C., Robock, A., and Ammann, C.: Volcanic forcing of climate over the past 1500 years: An
1008 improved ice core-based index for climate models, *Journal of Geophysical Research: Atmospheres*,
1009 113, n/a-n/a, 10.1029/2008JD010239, 2008.

1010 Gentine, P., Holtslag, A. A. M., D'Andrea, F., and Ek, M.: Surface and Atmospheric Controls on the
1011 Onset of Moist Convection over Land, *Journal of Hydrometeorology*, 14, 1443-1462, 10.1175/jhm-d-
1012 12-0137.1, 2013.

1013 Gleckler, P. J., Wigley, T. M. L., Santer, B. D., Gregory, J. M., AchutaRao, K., and Taylor, K. E.:
1014 Volcanoes and climate: Krakatoa's signature persists in the ocean, *Nature*, 439, 675-675, 2006.

1015 Grinsted, A., Moore, J. C., and Jevrejeva, S.: Application of the cross wavelet transform and wavelet
1016 coherence to geophysical time series, *Nonlin. Processes Geophys.*, 11, 561-566, 10.5194/npg-11-561-
1017 2004, 2004.

1018 Gunnarson, B. E., Linderholm, H. W., and Moberg, A.: Improving a tree-ring reconstruction from
1019 west-central Scandinavia: 900 years of warm-season temperatures, *Climate Dynamics*, 36, 97-108,
1020 10.1007/s00382-010-0783-5, 2011.

1021 Haarsma, R. J., Selden, F., Hurk, B. v., Hazeleger, W., and Wang, X.: Drier Mediterranean soils due to
1022 greenhouse warming bring easterly winds over summertime central Europe, *Geophysical Research*
1023 *Letters*, 36, n/a-n/a, 10.1029/2008GL036617, 2009.

1024 Harris, I., Jones, P. D., Osborn, T. J., and Lister, D. H.: Updated high-resolution grids of monthly
1025 climatic observations – the CRU TS3.10 Dataset, *International Journal of Climatology*, 34, 623-642,
1026 10.1002/joc.3711, 2014.

1027 Haurwitz, M. W., and Brier, G. W.: A Critique of the Superposed Epoch Analysis Method: Its
1028 Application to Solar–Weather Relations, *Monthly Weather Review*, 109, 2074-2079, 10.1175/1520-
1029 0493(1981)109<2074:acotse>2.0.co;2, 1981.

1030 Hegerl, G. C., Black, E., Allan, R. P., Ingram, W. J., Polson, D., Trenberth, K. E., Chadwick, R. S.,
1031 Arkin, P. A., Sarojini, B. B., Becker, A., Dai, A., Durack, P. J., Easterling, D., Fowler, H. J., Kendon,
1032 E. J., Huffman, G. J., Liu, C., Marsh, R., New, M., Osborn, T. J., Skliris, N., Stott, P. A., Vidale, P.-L.,
1033 Wijffels, S. E., Wilcox, L. J., Willett, K. M., and Zhang, X.: Challenges in Quantifying Changes in the
1034 Global Water Cycle, *Bulletin of the American Meteorological Society*, 96, 1097-1115, 10.1175/bams-
1035 d-13-00212.1, 2015.

1036 Helama, S., and Lindholm, M.: Droughts and rainfall in south eastern Finland since AD 874, inferred
1037 from Scots pine tree-rings, *Boreal Environ Res*, 8, 171-183, 2003.

1038 Helama, S., Merilainen, J., and Tuomenvirta, H.: Multicentennial megadrought in northern Europe
1039 coincided with a global El Nino-Southern Oscillation drought pattern during the Medieval Climate
1040 Anomaly, *Geology*, 37, 175-178, 10.1130/g25329a.1, 2009.

1041 Held, I. M., and Soden, B. J.: Robust Responses of the Hydrological Cycle to Global Warming,
1042 *Journal of Climate*, 19, 5686-5699, 10.1175/jcli3990.1, 2006.

1043 Iles, C. E., Hegerl, G. C., Schurer, A. P., and Zhang, X.: The effect of volcanic eruptions on global
1044 precipitation, *Journal of Geophysical Research: Atmospheres*, 118, 8770-8786, 10.1002/jgrd.50678,
1045 2013.

1046 Iles, C. E., and Hegerl, G. C.: Systematic change in global patterns of streamflow following volcanic
1047 eruptions, *Nature Geoscience*, 8, 838-842, 10.1038/ngeo2545, 2015.

1048 Jones, P. D., Osborn, T. J., and Briffa, K. R.: Estimating Sampling Errors in Large-Scale Temperature
1049 Averages, *Journal of Climate*, 10, 2548-2568, 10.1175/1520-0442(1997)010<2548:eseils>2.0.co;2,
1050 1997.

1051 Jones, P. D., and Lister, D. H.: The influence of the circulation on surface temperature and
1052 precipitation patterns over Europe, *Clim. Past*, 5, 259-267, 10.5194/cp-5-259-2009, 2009.

1053 Jones, P. D., Melvin, T. M., Harpham, C., Grudd, H., and Helama, S.: Cool North European summers
1054 and possible links to explosive volcanic eruptions, *Journal of Geophysical Research: Atmospheres*,
1055 118, 6259-6265, 10.1002/jgrd.50513, 2013.

1056 Jönsson, K., and Nilsson, C.: Scots Pine (*pinus sylvestris*L.) on Shingle Fields: A Dendrochronologic
1057 Reconstruction of Early Summer Precipitation in Mideast Sweden, *Journal of Climate*, 22, 4710-4722,
1058 10.1175/2009jcli2401.1, 2009.

1059 Jungclaus, J. H., Lohmann, K., and Zanchettin, D.: Enhanced 20th-century heat transfer to the Arctic
1060 simulated in the context of climate variations over the last millennium, *Clim. Past*, 10, 2201-2213,
1061 10.5194/cp-10-2201-2014, 2014.

1062 Kavvada, A., Ruiz-Barradas, A., and Nigam, S.: AMO's structure and climate footprint in
1063 observations and IPCC AR5 climate simulations, *Climate Dynamics*, 41, 1345-1364, 10.1007/s00382-
1064 013-1712-1, 2013.

1065 Landrum, L., Otto-Bliesner, B. L., Wahl, E. R., Conley, A., Lawrence, P. J., Rosenbloom, N., and
1066 Teng, H.: Last Millennium Climate and Its Variability in CCSM4, *Journal of Climate*, 26, 1085-1111,
1067 10.1175/JCLI-D-11-00326.1, 2012.

1068 Lehner, F., Joos, F., Raible, C. C., Mignot, J., Born, A., Keller, K. M., and Stocker, T. F.: Climate and
1069 carbon cycle dynamics in a CESM simulation from 850 to 2100 CE, *Earth Syst. Dynam.*, 6, 411-434,
1070 10.5194/esd-6-411-2015, 2015.

1071 Linderholm, H., and Molin, T.: Early nineteenth century drought in east central Sweden inferred from
1072 dendrochronological and historical archives, *Climate Research*, 29, 63-72, 2005.

1073 Linderholm, H. W., Niklasson, M., and Molin, T.: Summer Moisture Variability in East Central
1074 Sweden Since the Mid-Eighteenth Century Recorded in Tree Rings, *Geografiska Annaler: Series A,*
1075 *Physical Geography*, 86, 277-287, 10.1111/j.0435-3676.2004.00231.x, 2004.

1076 Linderholm, H. W., Björklund, J., Seftigen, K., Gunnarson, B. E., Grudd, H., Jeong, J.-H., Drobyshv,
1077 I., and Liu, Y.: Dendroclimatology in Fennoscandia – from past accomplishments to future potential,
1078 *Climate of the Past*, 6, 93-114, 2010.

1079 Linderholm, H. W., Björklund, J., Seftigen, K., Gunnarson, B. E., and Fuentes, M.: Fennoscandia
1080 revisited: a spatially improved tree-ring reconstruction of summer temperatures for the last 900 years,
1081 *Climate Dynamics*, 45, 933-947, 10.1007/s00382-014-2328-9, 2014.

1082 Madden, R. A., and Williams, J.: The Correlation between Temperature and Precipitation in the
1083 United States and Europe, *Monthly Weather Review*, 106, 142-147, 10.1175/1520-
1084 0493(1978)106<0142:tcbtap>2.0.co;2, 1978.

1085 McCarroll, D., Loader, N. J., Jalkanen, R., Gagen, M. H., Grudd, H., Gunnarson, B. E., Kirchhefer, A.
1086 J., Friedrich, M., Linderholm, H. W., Lindholm, M., Boettger, T., Los, S. O., Remmele, S., Kononov,
1087 Y. M., Yamazaki, Y. H., Young, G. H., and Zorita, E.: A 1200-year multiproxy record of tree growth
1088 and summer temperature at the northern pine forest limit of Europe, *The Holocene*, 23, 471-484,
1089 10.1177/0959683612467483, 2013.

1090 Melvin, T. M., and Briffa, K. R.: A “signal-free” approach to dendroclimatic standardisation,
1091 *Dendrochronologia*, 26, 71-86, 10.1016/j.dendro.2007.12.001, 2008.

1092 National Research Council: *Surface Temperature Reconstructions for the Last 2,000 Years*, The
1093 National Academies Press, Washington, DC978-0-309-10225-4, 160, 2006.

1094 Oglesby, R., Feng, S., Hu, Q., and Rowe, C.: The role of the Atlantic Multidecadal Oscillation on
1095 medieval drought in North America: Synthesizing results from proxy data and climate models, *Global*
1096 *Planet Change*, 84–85, 56-65, <http://dx.doi.org/10.1016/j.gloplacha.2011.07.005>, 2012.

1097 Osborn, T. J.: Simulating the winter North Atlantic Oscillation: the roles of internal variability and
1098 greenhouse gas forcing, *Climate Dynamics*, 22, 605-623, 10.1007/s00382-004-0405-1, 2004.

1099 Otto-Bliesner, B. L., Brady, E. C., Fasullo, J., Jahn, A., Landrum, L., Stevenson, S., Rosenbloom, N.,
1100 Mai, A., and Strand, G.: Climate Variability and Change since 850 CE: An Ensemble Approach with
1101 the Community Earth System Model, *Bulletin of the American Meteorological Society*, 97, 735-754,
1102 10.1175/bams-d-14-00233.1, 2016.

1103 Sarojini, B. B., Stott, P. A., and Black, E.: Detection and attribution of human influence on regional
1104 precipitation, *Nature Clim. Change*, 6, 669-675, 10.1038/nclimate2976, 2016.

1105 Schmidt, G. A., Jungclaus, J. H., Ammann, C. M., Bard, E., Braconnot, P., Crowley, T. J., Delaygue,
1106 G., Joos, F., Krivova, N. A., Muscheler, R., Otto-Bliesner, B. L., Pongratz, J., Shindell, D. T., Solanki,
1107 S. K., Steinhilber, F., and Vieira, L. E. A.: Climate forcing reconstructions for use in PMIP

1108 simulations of the last millennium (v1.0), *Geosci. Model Dev.*, 4, 33-45, 10.5194/gmd-4-33-2011,
1109 2011.

1110 Seftigen, K., Linderholm, H. W., Drobyshev, I., and Niklasson, M.: Reconstructed drought variability
1111 in southeastern Sweden since the 1650s, *International Journal of Climatology*, 33, 2449-2458,
1112 10.1002/joc.3592, 2013.

1113 Seftigen, K., Björklund, J., Cook, E. R., and Linderholm, H. W.: A tree-ring field reconstruction of
1114 Fennoscandian summer hydroclimate variability for the last millennium, *Climate Dynamics*, 44, 3141-
1115 3154, 10.1007/s00382-014-2191-8, 2014.

1116 Seftigen, K., Cook, E., Linderholm, H., Fuentes, M., and Björklund, J.: The Potential of Deriving
1117 Tree-Ring-Based Field Reconstructions of Droughts and Pluvials over Fennoscandia, *Journal of*
1118 *Climate*, 28, 3453-3471, 10.1175/JCLI-D-1300734.s1, 2015.

1119 Seneviratne, S. I., Corti, T., Davin, E. L., Hirschi, M., Jaeger, E. B., Lehner, I., Orlowsky, B., and
1120 Teuling, A. J.: Investigating soil moisture–climate interactions in a changing climate: A review, *Earth-*
1121 *Science Reviews*, 99, 125-161, <http://dx.doi.org/10.1016/j.earscirev.2010.02.004>, 2010.

1122 Shindell, D. T., Schmidt, G. A., Mann, M. E., and Faluvegi, G.: Dynamic winter climate response to
1123 large tropical volcanic eruptions since 1600, *Journal of Geophysical Research: Atmospheres*, 109, n/a-
1124 n/a, 10.1029/2003JD004151, 2004.

1125 Sigl, M., Winstrup, M., McConnell, J. R., Welten, K. C., Plunkett, G., Ludlow, F., Buntgen, U.,
1126 Caffee, M., Chellman, N., Dahl-Jensen, D., Fischer, H., Kipfstuhl, S., Kostick, C., Maselli, O. J.,
1127 Mekhaldi, F., Mulvaney, R., Muscheler, R., Pasteris, D. R., Pilcher, J. R., Salzer, M., Schupbach, S.,
1128 Steffensen, J. P., Vinther, B. M., and Woodruff, T. E.: Timing and climate forcing of volcanic
1129 eruptions for the past 2,500 years, *Nature*, 523, 543-549, 2015.

1130 Taylor, K. E., Stouffer, R. J., and Meehl, G. A.: An Overview of CMIP5 and the Experiment Design,
1131 *Bulletin of the American Meteorological Society*, 93, 485-498, 10.1175/bams-d-11-00094.1, 2012.

1132 Thiéblemont, R., Matthes, K., Omrani, N.-E., Kodera, K., and Hansen, F.: Solar forcing synchronizes
1133 decadal North Atlantic climate variability, *Nature communications*, 6, 8268, 2015.

1134 Thomson, D. J.: Spectrum estimation and harmonic analysis, *Proceedings of the IEEE*, 70, 1055-1096,
1135 10.1109/PROC.1982.12433, 1982.

1136 Thornthwaite, C. W.: An Approach Toward a Rational Classification of Climate, *Soil Science*, 66, 77,
1137 1948.

1138 Tolwinski-Ward, S., Evans, M. N., Hughes, M. K., and Anchukaitis, K. J.: An efficient forward model
1139 of the climate controls on interannual variation in tree-ring width, *Climate Dynamics*, 36, 2419-2439,
1140 10.1007/s00382-010-0945-5, 2011.

1141 Trenberth, K. E.: Changes in precipitation with climate change, *Climate Research*, 47, 123-138,
1142 10.3354/cr00953, 2011.

1143 van Oldenborgh, G. J., and Van Ulden, A. A. D.: On the relationship between global warming, local
1144 warming in the Netherlands and changes in circulation in the 20th century, *International Journal of*
1145 *Climatology*, 23, 1711-1724, 10.1002/joc.966, 2003.

1146 Vicente-Serrano, S. M., Beguería, S., and López-Moreno, J. I.: A Multiscalar Drought Index Sensitive
1147 to Global Warming: The Standardized Precipitation Evapotranspiration Index, *Journal of Climate*, 23,
1148 1696-1718, 10.1175/2009jcli2909.1, 2010.

1149 Vicente-Serrano, S. M., Gouveia, C., Camarero, J. J., Beguería, S., Trigo, R., López-Moreno, J. I.,
1150 Azorín-Molina, C., Pasho, E., Lorenzo-Lacruz, J., Revuelto, J., Morán-Tejeda, E., and Sanchez-
1151 Lorenzo, A.: Response of vegetation to drought time-scales across global land biomes, *Proceedings of*
1152 *the National Academy of Sciences*, 110, 52-57, 10.1073/pnas.1207068110, 2013.

1153 Watanabe, S., Hajima, T., Sudo, K., Nagashima, T., Takemura, T., Okajima, H., Nozawa, T., Kawase,
1154 H., Abe, M., Yokohata, T., Ise, T., Sato, H., Kato, E., Takata, K., Emori, S., and Kawamiya, M.:
1155 MIROC-ESM 2010: model description and basic results of CMIP5-20c3m experiments, *Geosci.*
1156 *Model Dev.*, 4, 845-872, 10.5194/gmd-4-845-2011, 2011.

1157 Wigley, T. M. L., Briffa, K. R., and Jones, P. D.: On the Average Value of Correlated Time Series,
1158 with Applications in Dendroclimatology and Hydrometeorology, *Journal of Climate and Applied*
1159 *Meteorology*, 23, 201-213, 10.1175/1520-0450(1984)023<0201:otavoc>2.0.co;2, 1984.

1160 Wilson, R., Miles, D., Loader, N. J., Melvin, T., Cunningham, L., Cooper, R., and Briffa, K.: A
1161 millennial long March–July precipitation reconstruction for southern-central England, *Climate*
1162 *Dynamics*, 10.1007/s00382-012-1318-z, 2012.

1163 Wilson, R., Anchukaitis, K., Briffa, K. R., Büntgen, U., Cook, E., D'Arrigo, R., Davi, N., Esper, J.,
1164 Frank, D., Gunnarson, B., Hegerl, G., Helama, S., Klesse, S., Krusic, P. J., Linderholm, H. W.,
1165 Myglan, V., Osborn, T. J., Rydval, M., Schneider, L., Schurer, A., Wiles, G., Zhang, P., and Zorita, E.:
1166 Last millennium northern hemisphere summer temperatures from tree rings: Part I: The long term
1167 context, *Quaternary Science Reviews*, 134, 1-18, 10.1016/j.quascirev.2015.12.005, 2016.
1168 Wu, P., Christidis, N., and Stott, P.: Anthropogenic impact on Earth/'s hydrological cycle, *Nature*
1169 *Clim. Change*, 3, 807-810, 2013.
1170 Wu, T., Song, L., Li, W., Wang, Z., Zhang, H., Xin, X., Zhang, Y., Zhang, L., Li, J., Wu, F., Liu, Y.,
1171 Zhang, F., Shi, X., Chu, M., Zhang, J., Fang, Y., Wang, F., Lu, Y., Liu, X., Wei, M., Liu, Q., Zhou,
1172 W., Dong, M., Zhao, Q., Ji, J., Li, L., and Zhou, M.: An overview of BCC climate system model
1173 development and application for climate change studies, *Journal of Meteorological Research*, 28, 34-
1174 56, 10.1007/s13351-014-3041-7, 2014.
1175 Zhang, H., Yuan, N., Esper, J., Werner, J. P., Xoplaki, E., Büntgen, U., Treydte, K., and Luterbacher,
1176 J.: Modified climate with long term memory in tree ring proxies, *Environmental Research Letters*, 10,
1177 084020, 10.1088/1748-9326/10/8/084020, 2015.
1178 Zhang, X., Zwiers, F. W., Hegerl, G. C., Lambert, F. H., Gillett, N. P., Solomon, S., Stott, P. A., and
1179 Nozawa, T.: Detection of human influence on twentieth-century precipitation trends, *Nature*, 448, 461-
1180 465, 2007.

1181

1182

1183

1184 **Tables and figures**

1185 **Table I.** CMIP5/PMIP3 model description.

Model Name	Resolution [Atmosphere]	Resolution [Ocean]	Reference
CCSM4	192 x 288	384 x 320	Landrum et al. (2012)
CESM1	96 x 144	384 x 320	Lehner et al. (2015)
IPSL-CM5A-LR	96 x 96	149 x 182	Dufresne et al. (2013)
MIROC-ESM	64 x 128	192 x 256	Watanabe et al. (2011)
MPI-ESM-P	96 x 192	220 x 256	Jungclaus et al. (2014)
BCC-CSM1-1	64 x 128	232 x 360	Wu et al. (2014)

1186 **Table II:** Tree-ring network description.

Site	Coord.	Time coverage	Standardization method	MSL ³	Source
Eastern Finland	61.87N, 28.90E	535 -2002 CE	RCS ¹	147 yrs	Helama et al. (2009) Online resource: http://lustiag.pp.fi/Saima/dendrotieto.htm Date access: January 2013
Gotland Sweden	57.49N, 18.41E	1127-2011 CE	RCS	130 yrs	Investigator: Schweingruber, F.H. Online resource: https://www.ncdc.noaa.gov/paleo/study/4427 Date access: January 2013 Updated in Seftigen et al. (2015)
Jondalen Norway	59.71N, 9.53E	1185 -2011 CE	RCS	165 yrs	Investigator: Briffa, K. Online resource: https://www.ncdc.noaa.gov/paleo/study/2826 Date access: January 2013 Updated in Seftigen et al. (2015)
Baljåsen Sweden	59.04N, 12.27E	1686-2002 CE	SF2 ²	174 yrs	Seftigen et al. (2015)
Björbo Sweden	60.27N, 14.44E	1450-2011 CE	SF	177 yrs	Investigator: Axelson, T. Online resource: https://www.ncdc.noaa.gov/paleo/study/2667 Date access: January 2013
Ekhultebergen Sweden	57.45N, 13.50E	1705-2008 CE	SF1	215 yrs	Seftigen et al. (2015)
Fårhagsberget Sweden	58.08N, 16.14E	1621-2011 CE	SF1	262 yrs	Seftigen et al. (2015)
Helvetets håla Sweden	57.14N, 16.14E	1691-2011 CE	SF1	255 yrs	Seftigen et al. (2015)
Halle-Vagnaren Sweden	57.17N, 15.17E	1718-2009 CE	SF3	186 yrs	Seftigen et al. (2015)
Hornslandet Sweden	59.01N, 11.08E	1590-2011 CE	SF1	270 yrs	Seftigen et al. (2015)
Korphålorna Sweden	61.43N, 17.00E	1790-2011 CE	SF1	199 yrs	Seftigen et al. (2015)
Myrkaby Sweden	57.45N, 15.23E	1669-2011 CE	SF2	294 yrs	Seftigen et al. (2015)
Nämndö Sweden	59.52N, 16.56E	1582-1995 CE	SF1	123 yrs	Investigator: Larsson, L. Online resource: https://www.ncdc.noaa.gov/paleo/study/3869 Date access: January 2013
Valekleven-Ombo Sweden	59.11N, 18.41E	1578-2011 CE	SF1	225 yrs	Seftigen et al. (2015)
Putbergen Sweden	58.37N, 14.32E	1734-2008 CE	SF1	188 yrs	Seftigen et al. (2015)
Salboknös Sweden	59.11N, 16.55E	1486-2011 CE	SF2	357 yrs	Seftigen et al. (2015)
Särö Sweden	61.92N, 11.93E	1712-2002 CE	SF3	176 yrs	Seftigen et al. (2015)
Sisshammer Sweden	59.46N, 14.54E	1661-2003 CE	SF	74 yrs	Investigator: Andreason, T. Online resource: https://www.ncdc.noaa.gov/paleo/study/2663 Date access: January 2013
Skärmarbodabergen Sweden	57.51N, 11.93E	1600-2002 CE	SF3	160 yrs	Seftigen et al. (2015)
Skitåsen Sweden	59.09N, 18.02E	1672-2011 CE	SF2	285 yrs	Seftigen et al. (2015)
Skuleskogen Sweden	59.26N, 15.07E	1448-2011 CE	SF	181 yrs	Seftigen et al. (2015)
Sörknatten Sweden	59.22N, 15.29E	1762-2009 CE	SF3	197 yrs	Seftigen et al. (2015)
Tjurhults mosse Sweden	63.06N, 18.29E	1655-2011 CE	SF2	268 yrs	Seftigen et al. (2015)
Tjusthult Sweden	58.55N, 12.27E	1681-2011 CE	SF1	221 yrs	Seftigen et al. (2015)
Tyresta Sweden	59.52N, 14.71E	1609-2010 CE	SF1	198 yrs	Linderholm and Molin (2005) Updated in Seftigen et al. (2015)

1187 ¹ RCS: Regional Curve Standardization;

1188 ² SF: Signal-Free Standardization. The number after the abbreviation indicates the PCA cluster number (Fig. S2);

1189 ³MSL: Mean Segment Length.

1190 **Table III.** Event years used in the Superposed Epoch Analysis (Fig. 4). The event lists are composed
 1191 of the 20 strongest eruptions from each record.

Source	Event years (CE)
Gao et al. (2008) (sulfate aerosol > 15 Tg)	1167, 1176, 1195, 1227, 1258, 1284, 1328, 1452, 1459, 1584, 1600, 1641, 1719, 1783, 1809, 1815, 1831, 1835, 1991
Crowley and Unterman (2013) (AOD > 0.13)	1229, 1258, 1259, 1286, 1287, 1456, 1457, 1600, 1601, 1641, 1695, 1696, 1809, 1810, 1815, 1816, 1817, 1884, 1992
Sigl et al. (2015) (global forcing < 5.86 W/m ²)	1108, 1171, 1191, 1230, 1258, 1276, 1286, 1345, 1453, 1458, 1601, 1641, 1695, 1783, 1809, 1815, 1832, 1836, 1992

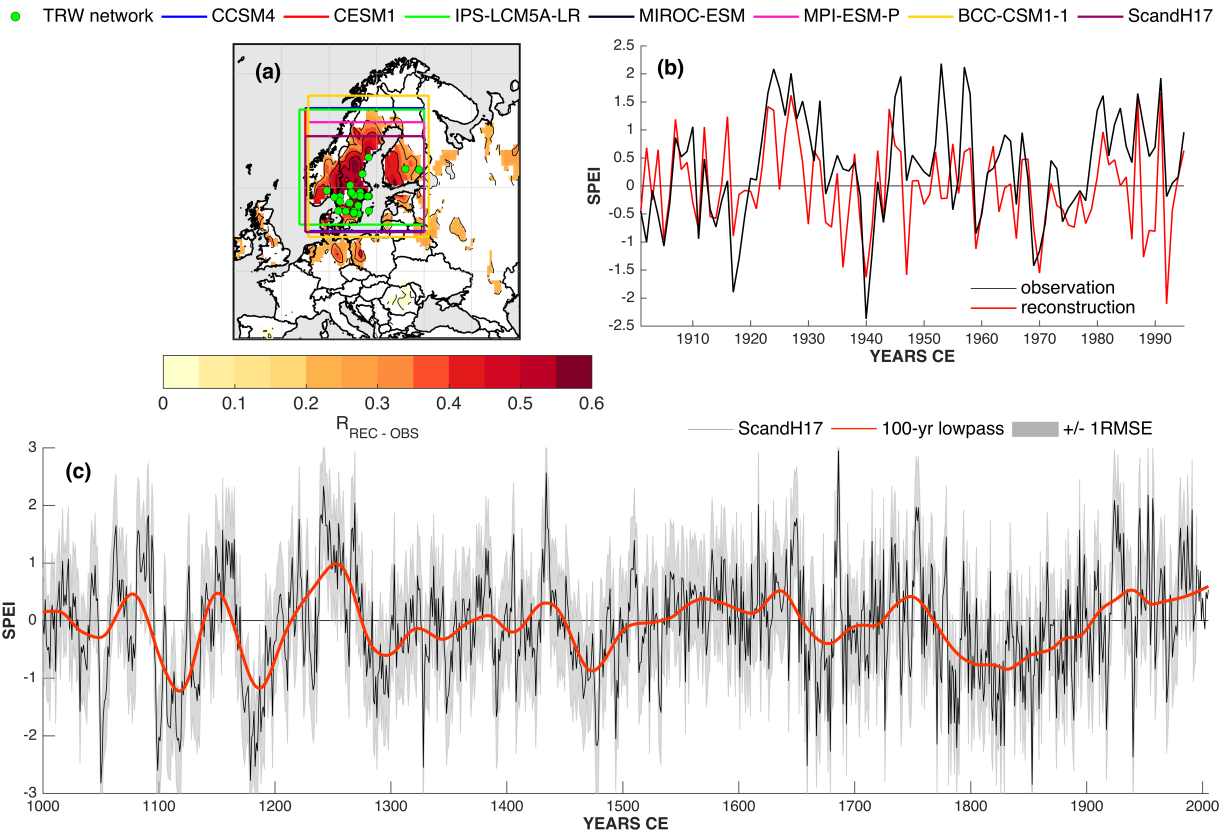


Figure 1: Average regional warm-season SPEI time series reconstructed from tree-rings. (a) Location of the tree-ring network used for regional reconstruction and the extent of the CMIP5/PMIP3 model precipitation and temperature grids used to derive regional SPEI estimates. Shaded contours display the correlation ($p < 0.1$) between the tree-ring reconstruction and fields of instrumental SPEI data over the 1901-1995 period; (b) average regional reconstructed and instrumental 20th century 2-month June SPEI; (c) average regional SPEI nested reconstruction, with the ± 1 RMSE of the regression equations outlined in grey shading. A smoothed version of the reconstruction using a 100-year loess smooth is shown in red. Reconstruction assessment metrics are provided in supplementary materials (Fig. S4).

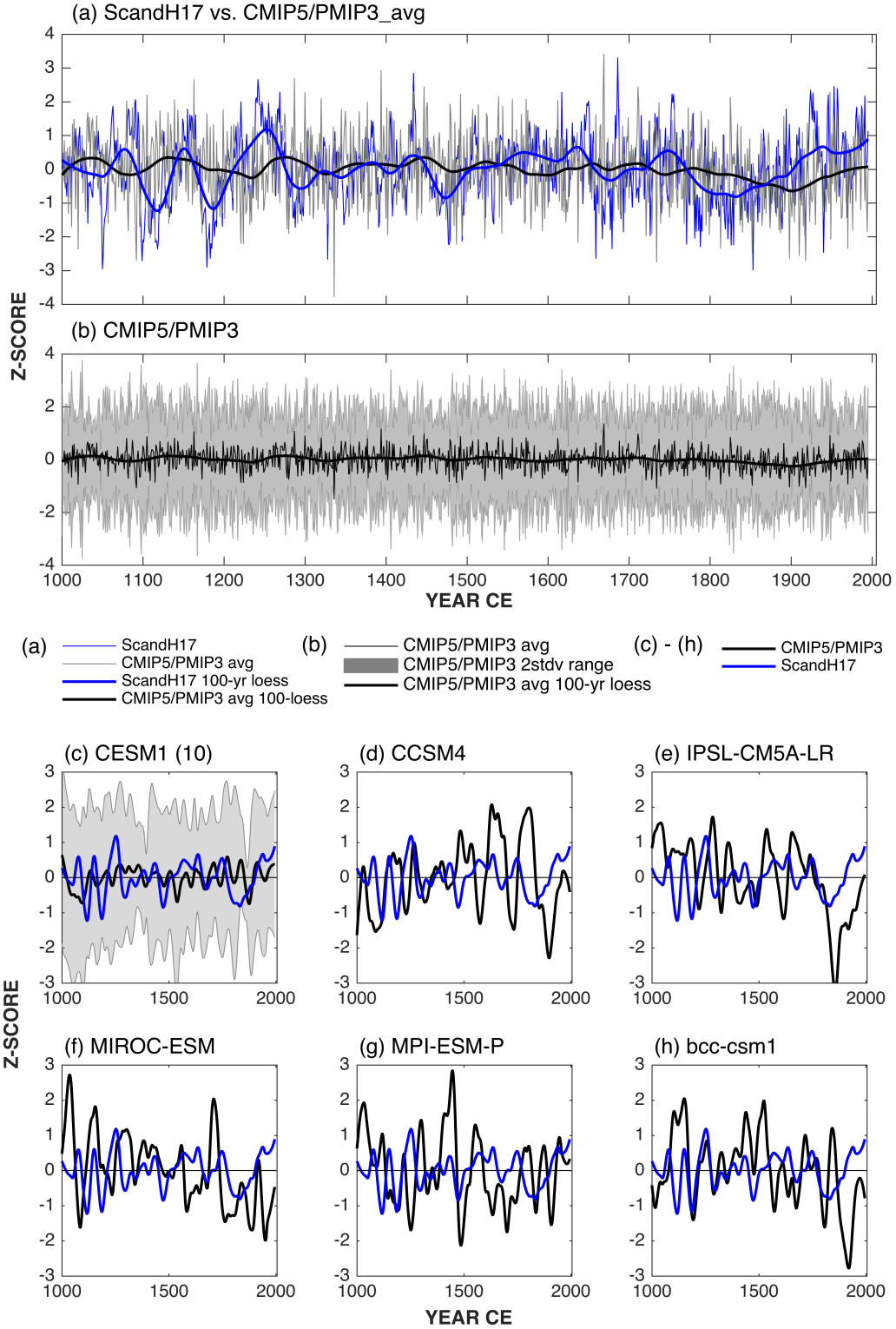


Figure 2: Comparison of reconstructed SPEI with forced model runs. (a) The reconstruction versus the mean of the six CMIP5/PMIP3 models transformed into standard normal deviates (z-scores) over the 1000-1995 CE period and smoothed with 100-year loess filter; (b) multimodel mean and the two standard deviation range (shading) of the six GCMs; (c) mean and two standard deviation (shading) of CESM1 ten smoothed and z-scored ensemble members (blue) together; (d) – (h) the

reconstruction (blue) versus individual model runs (black). All time series have been smoothed with 100-year loess filter and then z-scored over the 1000-1995 CE period.

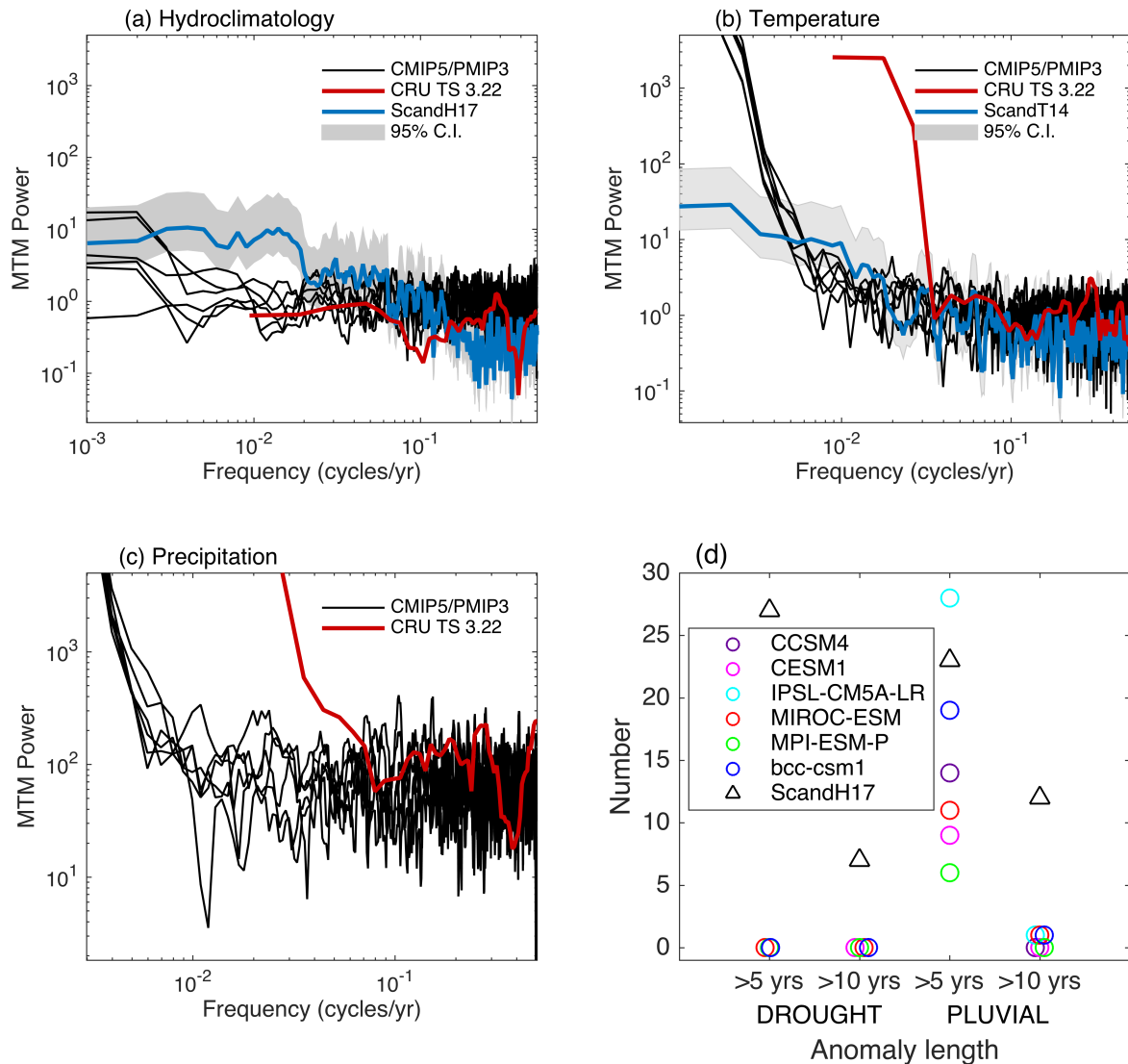


Figure 3: Spectral properties (multi-taper approach, 4 tapers) of (a) SPEI, (b) temperature and (c) precipitation over the common 1100-1995 period. For SPEI and temperature, the spectral properties of individual GCMs (r1i1p1 ensemble) are compared to those of the tree-ring ScandH17 and ScandT14 reconstructions and regionally averaged instrumental CRU TS 3.22 data. Shaded areas show the 95% confidence interval of the reconstruction spectra. (d) The number of droughts and pluvials in the reconstructed and simulated time series that are > 5 and >10 years in duration. Spectral properties of the individual models are provided in Fig. S7.

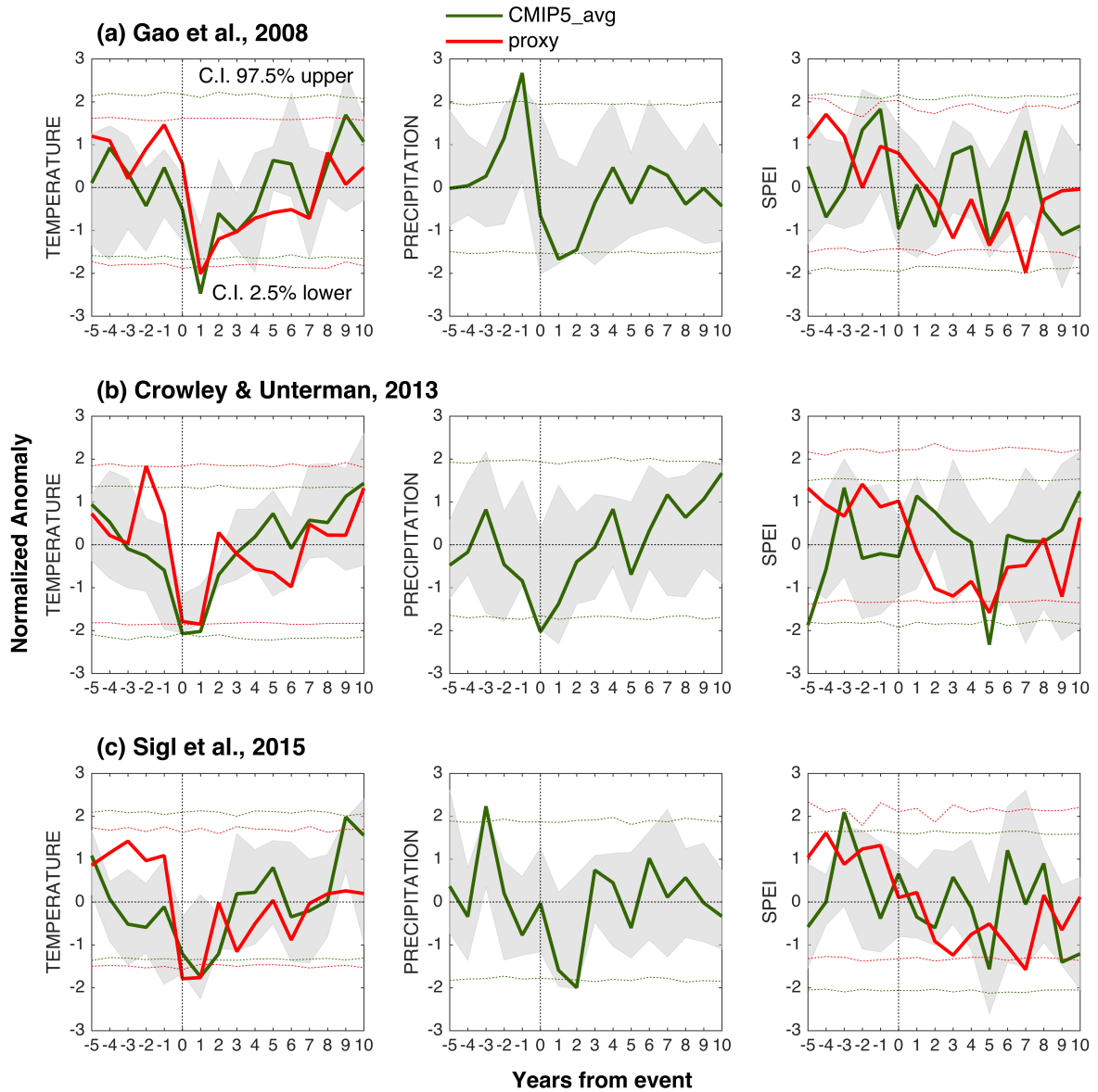


Figure 4: Modeled and reconstructed hydroclimate response to eruptions. Superposed epoch analysis using the 20 largest eruption years from the (a) Gao et al. (2008), (b) Crowley and Unterman (2013), and (c) Sigl et al. (2015). Table III lists the event years used in the analysis. Grey shading indicate the range of modeled hydroclimate response from the six GCMs. Confidence intervals (C.I.) are derived from bootstrap resampling ($N = 10\,000$).

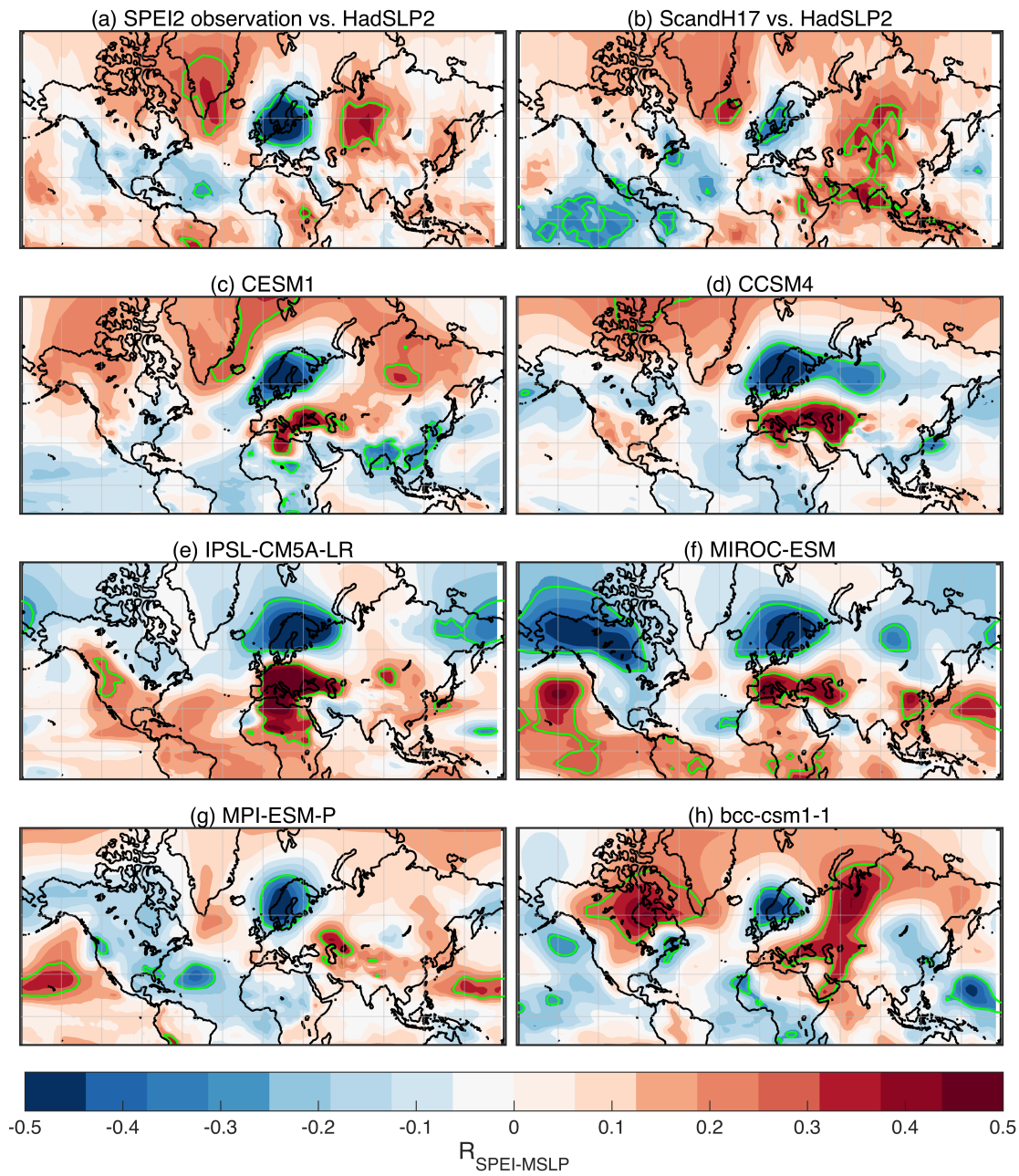


Figure 5: Spatial distribution of correlation coefficient of northern European warm season hydroclimate and mean sea level pressure (MSLP). Association between regional drought index and sea level pressure over the 1950-1995 period. (a) observational, (b) ScandH17, (c)-(g) model based results (including r1i1p1 ensemble only). Regions with significant ($p < 0.05$) correlations are outlined in green contours.

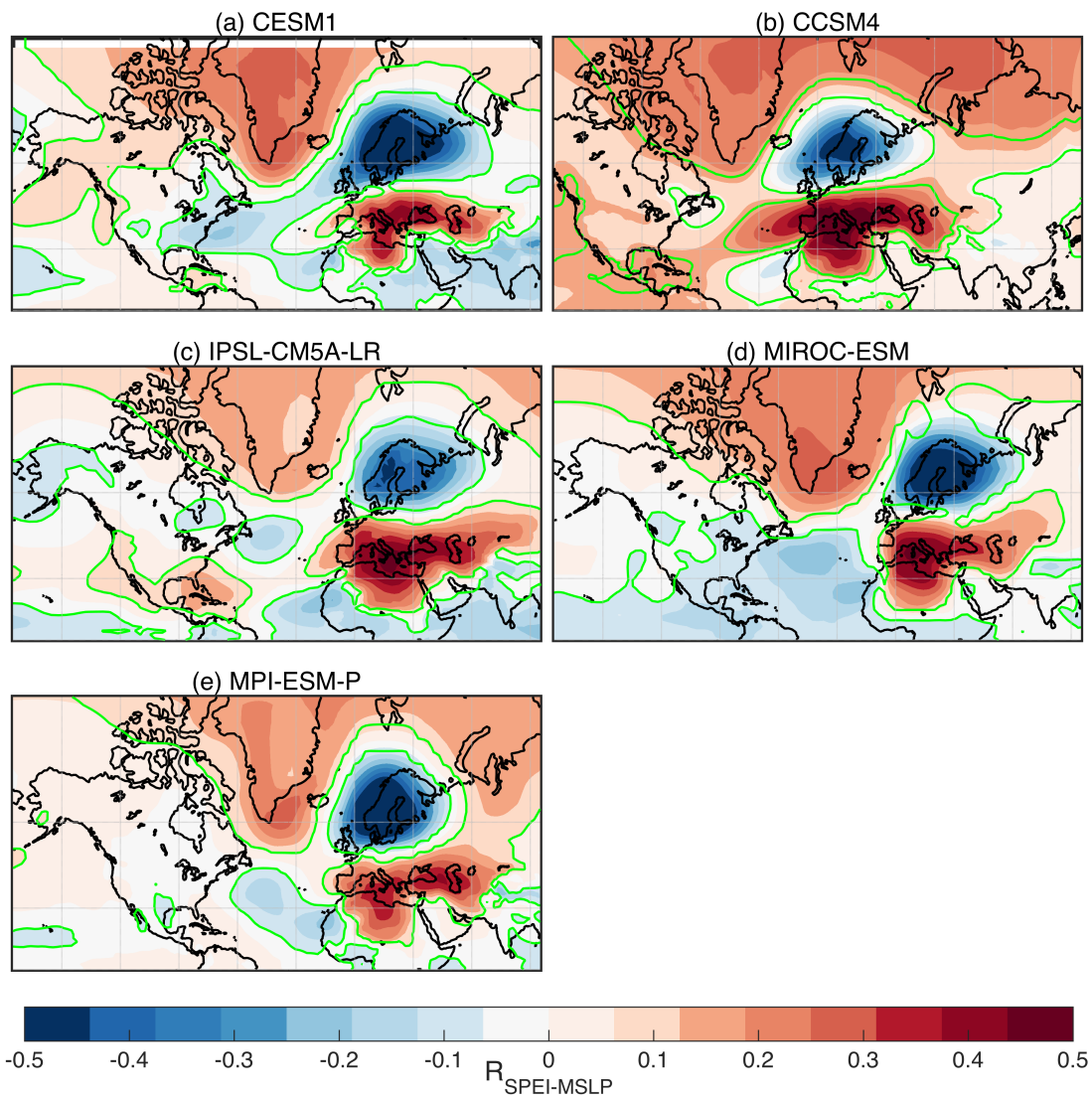


Figure 6: Spatial distribution of correlation coefficient of northern European warm season hydroclimate and mean sea level pressure (MSLP). Same as Fig. 5, but for the 850-1849 CE period.

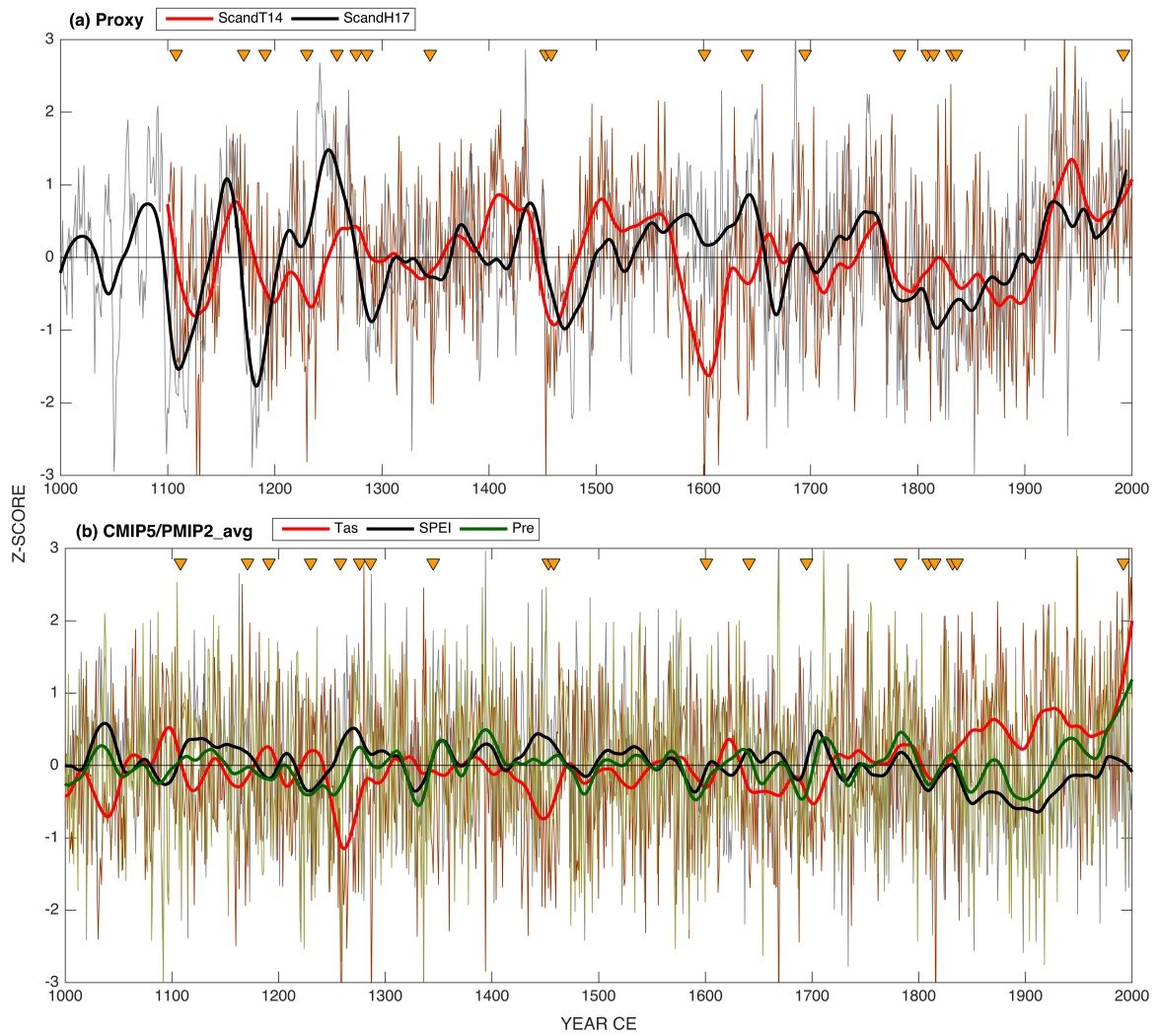


Figure 7: Time series of (a) ScandH17 and ScandT14, and (b) GCM (r1i1p1 ensemble) average temperature, precipitation and SPEI. Smoothed time-series using a 50-year loess filter are shown as thick lines. Individual model data are provided in supplementary material (Fig. S8). The years with volcanic eruptions from Table III are indicated by triangle glyphs.

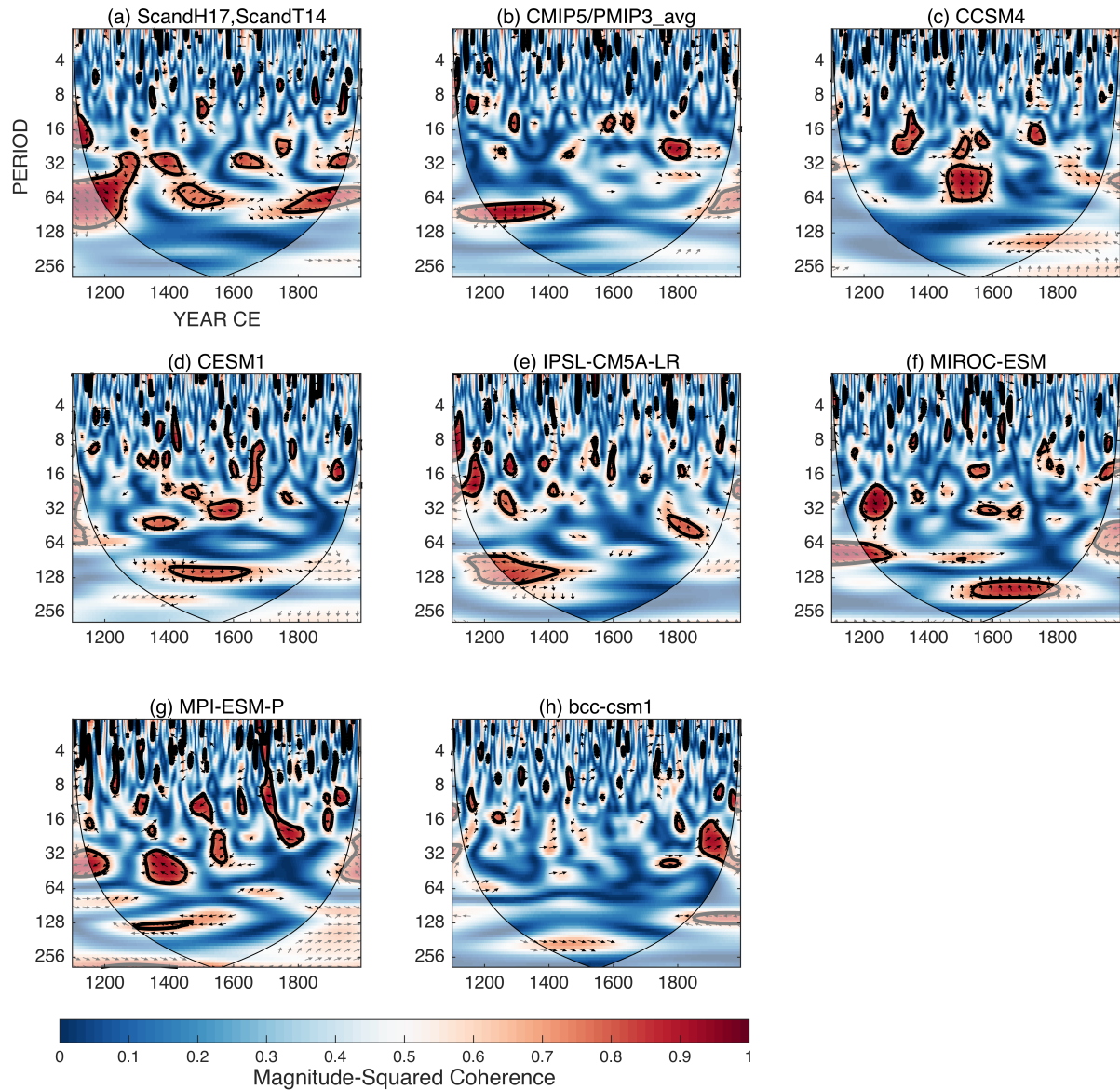


Figure 8: Squared wavelet coherence and phase between (a) ScandH17 and ScandT14, and (b) – (h) CMIP5/PMIP3 simulations of temperature and rainfall. The arrows indicate the relative phase relationship between two series; right (left) pointing arrow indicates in-phase (180 degrees out of phase) relationship. Significant coherence at 95% significance level is shown as thick contour.